CoA Note M & P No. 7.

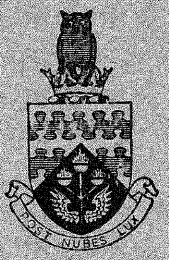

THE COLLEGE OF AERONAUTICS
CRANFIELD

ELECTRO - CHEMICAL MACHINING

by

D. A. Glew and C. F. Noble

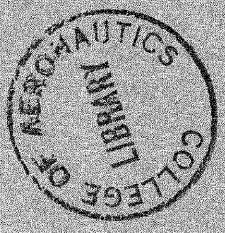

CoA Note M and P No. 7

February, 1965

THE COLLEGE OF AERONAUTICS

DEPARTMENT OF PRODUCTION AND INDUSTRIAL ADMINISTRATION

Electro-chemical machining

- by -

D.A. Glew and C.F. Noble*

SUMMARY

This report introduces the reader to the process and to the requirements which must be considered for its installation on the shop floor. Although only electro-chemical shaping is dealt with, many of the parameters investigated are fundamental to other configurations. The machining characteristics of several high strength alloys and die steels have been investigated; also of aluminium and mild steel. Electrolyte heating effects and the physical attributes of the machined surface have been considered. Electrode and workpiece shapes have been simulated for static field examinations and these followed by investigations under dynamic machining conditions.

* This Note is based partly on a thesis submitted by the first author in partial fulfillment of the requirements for the Diploma of Advanced Engineering, 1963.

Contents

Introduction

Electro-chemical machining involves the controlled removal of metal from a workpiece by electrolysis under high current density, low potential conditions. In many ways the process is a competitor to spark-discharge machining, but the action is entirely different.

When the spark-discharge machining, a potential is built up across the working gap until the dielectric characteristic of the liquid used breaks down and a localised spark passes across the ionised gap. The metal is locally vapourised in a manner akin to a miniature explosion and the surface is then rapidly quenched by the dielectric, so causing residual tensile surface stresses. A succession of sparks erode the surface of the workpiece and, to a lesser extent, the surface of the electrode.

When electro-chemical machining, a liquid electrolyte passes through the gap between a negative electrode and a positive workpiece. Consequently current flows continuously at a density depending on the length of the current path, the conductivity of the electrolyte and the applied potential. The surface of the workpiece is thus machined by high-speed electrolysis. The electrode is not machined and plating of its surface is prevented by the combination of a high electrolyte flow rate and a low potential difference. Therefore, some of the problems associated with spark-discharge machining do not appear. However, the process is not free from difficulties, not least of which is the necessity of ensuring a homogenious electrolyte flow and, for two and three dimensionally shaped surfaces, allowing for variations in current density distribution when determining the shape of the electrode.

Most conventional metal cutting operations could be converted to E.C.M. but this report is devoted entirely to the technique of forming components which would most probably be machined conventionally by die sinking techniques. Research and development of this process has been fairly active in America, most notably by the Batelle Memorial Institute, Anocut Co., of Chicago and the Cincinacti Milling Machine Co. Several groups in Britain have undertaken research while machines have been developed for the market by Metachemical Machines Ltd., of Crawley, Sussex, and by Rolls-Royce Ltd., Derby.

A Merkem Shaping Machine has been used for the research reported herein, see Figures 1 and 2. This machine is equipped with a transformer/rectifier power unit capable of 500 amp. output to two moving cathode electrodes. The electrode feed is operated independently from an infinitely variable pneumatic system while the electrolyte, which is contained in a plastic tank, is fed to the working area through a centrifugal pump with a bypass valve for the flow control. Simplicity has been the aim of the designers of this machine and consequently initial price and maintenance costs are comparatively low. For convenience during the investigations the machine was adjusted for single moving cathode use with the other cathode converted to a static anode upon which to fix the work.

The Barmax (Rolls Royce) machine has four machining heads each capable of carrying 1,000 amps. Electrode feed is obtained from an hydraulic system having a current control system to regulate the size of the machining gap. No attempt is made in this report to examine a control system and it will remain the duty of potential users to make their own decision. The authors consider it sufficient to warn the reader against confusion with the need for feed-back control when spark-machining and to draw attention to the fact that numerous E.C.M. units without feed-back control are being used quite successfully in industry.

One of the most important assets of E.C.M. is its ability to machine metals at rates which are independent of their hardness. This often places the process, both technically and economically, in a favourable position with conventional methods. An example can be quoted from experience gained at Bristol Siddeley Engines with P.E.11, an electric-arc, vacuum-melted, high temperature alloy, containing iron nickel, cobalt and chromium. Using profile milling methods to rough-form guide-vanes, cutter life varied between five and fifteen vanes. With E.C.M. methods floor to floor time was considerably reduced, surface-finish improved markedly, final tolerances were held to within .005 inch. and milling machines were released for other work.

One can reasonably expect that with the increasing need for high temperature, high tensile, hard materials, the scope for E.C.M. will become very wide.

E.C.M. and the shop-floor

The decision to purchase

A machine-tool is usually purchased for one of the following reasons:-

(a) replacement of existing plant,
(b) expansion of existing production facilities,
(c) changes in techniques in order to reduce component costs,
(d) new design developments requiring specialist machines.

Purchase will generally follow market evaluation based on experience, manufacturers guarantees, and after-sales service facilities. The machine will be installed in a condition suited to almost immediate production and operator training will usually be rapid owing to familiarity with the techniques involved.

The situation differs, however, when an E.C.M. facility is introduced. The reason for a purchase will be based almost entirely on combined technical and economic limitations of orthodox methods. The market will be small and the decision to purchase will follow either the mutual agreement of manufacturer and customer that the work envisaged is a feasible proposition or solely by the customer considering the machine as suitable for both applied research as well as for production use. Invariably a certain amount of delay in development and pre-production planning will be experienced before achieving satisfactory machining conditions. This period of inconvenience may be minimised if the supplier will accept responsibility for planning and especially if this service includes manufacture of cathode formers and operator training. However, the authors believe that to ensure maximum benefits a technical team should be formed to adapt and develop this extremely potential technique for efficient production use. Team work is emphasized by the interdependency of development engineer, jig and tool designer, electrical engineer, planning engineer and, in some instances, chemist.

Machine Installation

The complete machine plus ancilliary equipment usually comprises an electrical supply unit containing transformer and rectifier, an electrolyte tank, pump and filtration unit, hydrogen extraction unit and possibly a cooling plant. Sufficient space must be allowed for all these units and they must be situated for ease of accessibility and, in the case of the tank, for ease of filling and drainage. With a continuous electrolyte settling tank system space requirements will not be small and must be given early consideration - see Fig. 17. When planning the installation due regard should be paid to possible future expansion to prevent later inconvenience and duplication of accessories and tank areas.

When machining, the liberation of hydrogen at the cathode surface is sufficient to cause a rapid build-up of an explosive gas above the electrolyte in the collection tank. On testing for the rapidity of hydrogen formation in the tank it was found that an 80% Lower Explosive Limit mixture had formed within two minutes when not using the forced ventilation system. A hydrogen extraction plant is, therefore, a necessary, but fortunately simple, system in order to avoid dangerous conditions in the machining area and in the surrounding workshop.

The efficiency of the E.C.M. process

The process under consideration is essentially electrolysis in accelerated form in which metal removal characteristics are of prime importance as opposed to the deposition aspects of electro-plating. Faradays laws of electrolysis state that:

1) The mass of any substance liberated is proportional to the total quantity of electricity which passes.

2) The masses of different substances liberated by the same quantity of electricity are proportional to their chemical equivalents.

From the second law it is clear that once a standard electro-chemical equivalent is known all others can be determined. By international agreement the ampere is defined as that current which will liberate .0011183 gram of silver per second. Consequently, the ideal conditions for other materials can be calculated and used as a datum for evaluation of efficiency.

For investigation, commercially pure Aluminium was chosen because it was readily available and has a single valency of 3. Calculations for 100% efficiency based on the above are given in Appendix 1 and depicted graphically in Fig. 3. Experiments were carried out on the Metkem Shaper using specimens with a surface area of 3.175 x 1.25 sq. inches. The weight of each piece was noted before and after each 1 minute duration test. The current was varied between 250 and 500 amperes, corresponding to current density values of approximately 64 to 130 amps. per sq. in. Electrolyte flow was set for maximum rate.

The choice of the apparently short time interval was governed by two reasons. Firstly, the volumes of material removed in this interval were adequate for accurate measurement. Secondly, at this stage of the experimental programme, ventilation facilities had not been installed and prolonged tests constituted a hazard in the area owing to the cathodic generation of hydrogen (see Appendix 2).

The machining characteristics during these tests proved very reliable and it was found that consistent and satisfactory machining could be achieved at a workpiece/former gap of .008 inch. Results are tabulated in Appendix 1 and the machining rate curve is given in Figure 3. To the extent that the latter is of linear form, it agrees with the pre-stated laws of Faraday. However, the actual removal rates obtained over the current range considered are approximately 25% higher than those predicted by Faraday.

To consider this fully it is necessary to note that, although E.C.M. operates on the same principle as electro-plating, certain physical conditions

differ drastically:-

a) The different state of the electrolyte. Electro-plating relies on a virtually motionless fluid while with E.C.M. the electrolyte is subject to rapid flow rates under high pressure and temperature conditions.

b) Relative current-voltage requirements differ. Electro-plating uses low current density and comparatively high voltage while E.C.M. requires high current density for high removal rates and voltage is correspondingly low to discourage cathode plating.

c) Electrode gap distances for the two processes differ in the order of thousands to one.

d) Metal and solution ionization rates are higher when machining than when plating.

Aluminium, when subjected to anodic attack by an external E.M.F. in a chloride solution under favourable current density conditions, is considered to pass into solution as a chloride ion. There is, however, in any aqeous solution, the chance that hydroxl ions will be discharged at the anode surface in addition to the prime ions. This is especially to be expected in alkaline solutions. The metal surface then becomes covered with a film of insoluble hydroxide, which hinders the passage of current and retards errosion rates. Clearly, it has to be determined whether or not this film is adherent and continuous or loose and porous. In the presence of a chloride radical in an electrolyte it is known that the layer is formed in a loose, porous, non-protective, and easily removable form. However, under high current density conditions the hydroxl ions formed will increase and if allowed to build up will tend to cause anode 'passivity'.

From Ohm's Law, ionic migration is inversely proportional to the gap width 'ℓ' at constant voltage. Reference to Fig. 20 reveals that as current path-length decreases to values approaching .005 to .003 inch, the curve becomes asymptotic to the current axis, giving rise to a rapid increase in current values, limited only by extra-to-gap circuit resistance and supply system capacity. Under such conditions ionic activity rises rapidly and the film builds up quickly as a result. Fortunately, with E.C.M., the combined action of the chloride radical and the mechanically abrasive action of the continuous flow of electrolyte at high velocity must be adequate to remove the film and so enable the corrosive action of the electrolyte to assist the applied E.M.F. in removing metal from the anode workpiece. Support for this conclusion is obtained from Ref. 1, to quote: 'If the conditions are such as to preclude the formation of a protective film of the product of corrosion; continued attack upon these metals by neutral solutions is perfectly possible'.

It is doubtful, however, that this effect could be attributed to more

than a fraction of the high efficiency values experienced and the authors turn to the experiments of Turrentine (Ref. 5) for a more likely explanation. He discovered that with an aluminium anode in a sodium chloride solution more of the metal dissolved than expected, but that a corresponding amount of hydrogen gas was liberated at the anode so maintaining an overall balance of oxidation and reduction. Measurements indicated current efficiencies of about 118%. This phenomena is apparently not fully understood, but it is believed that the metal first ionises to some extent with a valency lower than normal; the ion thus formed is then unstable and reacts with water to give its normal charge, hydrogen being liberated in the process. This kind of mechanism is borne out by the fact that hydrogen evolution often continues for a short time after the current has stopped. Ref. 5, 6 and 7.

With the assumption that a similar action is taking place in the experiments reported herein, a proportion of the 100% efficiency calculations should have been based on a valency lower than 3 but the experimental work required before this can be apportioned correctly is beyond the scope of the present work, especially considering the interrelation of the other parameters peculiar to E.C.M.

Figure 3 records removal rates of aluminium when using different concentrations of sodium chloride solution and other neutral electrolytes. Note that the lower concentration electrolyte with 10.5% Na Cl gave the most efficient machining. As a result of workpiece surface observation after each test, the following reasoning is suggested in explanation.

Increase in the electrolyte solution enable the same charge to pass at lower field intensity values. Fig. 16 records the E.M.F./electrolyte concentration relationship for Na Cl solutions at two constant current density values with a constant gap setting. For concentrations up to approximately 26%, field intensity values fall. From Ohm's Law we know that the ionic migration rate diminishes as the ratio of E.M.F. to path length decreases and therefore as electrolyte concentration increases we must have a solution where the gap contains a larger number of slower moving ions. Consequently there is a tendency towards a thicker hydroxyl layer at the anode surface resulting in increased resistance to machining, although not necessarily causing removal rate to fall below the Faraday prediction. However, above approximately 26% concentrations the E.M.F. required to maintain charge level rises owing to oxygen liberation at the anode surface. This creates partial passivity conditions probably coincident with lower than Faraday machining rates.

The initial appearance of passivity tendencies is indicated by a fine oxide layer on the anode surface, the thickness of which increases in the direction of electrolyte flow. Should the stage be reached where oxygen

is being liberated it will be indicated by the current/voltage relationship, not on inspection of the workpiece surface since the then tenacious, oxide layer will be transparent.

A further consideration affecting process efficiency is electrolyte saturation. Naturally, the solubility of all substances is limited and given a sufficiently high current density the liquid next to the anode could become supersaturated with the anodic product. Clearly this condition is less likely to arise the more rapidly electrolyte replacement occurs.

The need for high electrolyte flow is obviously a requirement from a number of points of view if high removal rates at high efficiency levels are to be envisaged. Previous investigators who have consistently experienced lower than Faraday removal rates may well have been limited by their flow-rate. Figure 4 amply indicates anode passivity when machining aluminium and the authors believe that similar circumstances will exist for other materials though not at the same current density values.

The machining characteristics of high-strength alloys

With advancements in materials research, design techniques and technological knowledge, the applications for alloys with high temperature, high strength properties are increasing. This applies throughout industry but more particularly to those concerned with aerospace requirements. As a result of the high strength of these materials, shaping them to the required accuracies is becoming increasingly difficult despite advances in cutting tool techniques; low feed rates, small depths of cut and high rates of tool wear are lowering production rates drastically and thereby raising costs.

The position has now been reached where unconventional production techniques are being investigated and this section of the report is concerned with the suitability of E.C.M. for machining of such materials and included for assessment are three samples of die steel.

Specimens were obtained either from sources within the aircraft industry or from the manufacturers. Material specification are given in Appendix 4.

Metal removal rates were measured at 50 amp. intervals over a 200 to 500 amp. range. Removal rates were converted to cubic inches per minute after taking the difference in specimen weight before and after machining. The surface finish was recorded after each test using the Taylor-Hobson Talysurf, all readings being taken at 0.3 wavelength cut-off.

Material P.E.11

This alloy is an electric-arc vacuum-melted material, which, in its heat-treated form presents formidable machining problems. It has high temperature properties and as such is being used for engine stator vanes where temperatures can be expected of the order of 1250°C.

Three electrolytes were used for the tests; these were 10.5% Na Cl, 15.5% Na Cl solution and 21.0% Na NO_3 solution, all by weight.

Fig. 5 illustrates the results obtained for these three salt solutions. With 21.0% Sodium Nitrate and 10.5% Sodium Chloride solutions the removal rate/current relationship remains linear over the range considered. However, the machining rate with 15.5% sodium chloride begins to fall-off above 400 amps. This suggests that with this electrolyte, and under the gap and flow conditions prevailing, a current density value of approximately 100 amps/sq.in. is the maximum to allow.

Fig. 15 indicates no advantage in surface finish as the current density is increased, a consistent 19μ-inch being obtained.

Material Deloro X - 40

This is a very tough alloy with excellent 'hot-hard' properties which has uses for the manufacture of moving parts under high temperature conditions.

When machined at gaps of .008 inch. satisfactory results were obtained over the complete range of current densities available; the removal rate/current relationship is linear for each electrolyte, shown in Figure 6. The current density value at 450 amps is 190 amps/sq.inch.

Fig. 15 illustrates that surface finish improves with current density, dropping finally to 18μ-inch.

Material F.V.448

This is a chrome steel which is considered to be of general purpose application within the aircraft industry. Its applications embrace compressor blades and compressor rotors. Compressor blade batch sizes are usually fairly high and E.C.M. methods could prove economical after only a short production time.

Figure 7 illustrates the removal rate/current relationship between 250 amps and 450 amps. This represents a current density range of 79-140 amps. per sq. inch.

Figure 15 indicates a reasonable improvement in surface finish as current density is increased but is unlikely to drop below 40μ-inch.

The surface of each specimen was covered with a very thin, easily removable grey film of oxide after each test. This film did not interfere with machining efficiencies over the range considered and higher machining rates are obviously possible at the electrolyte flow rate available.

Note that the 15.5% Na Cl solution gives slightly higher machining rates than the 10.5% solution. Presumably the oxide is less tenacious with the additional strength of chloride radical.

Material - Jessop Saville G.64

This is an alloy steel which exhibits good casting characteristics, and which has high-temperature, high-strength properties. It is very expensive and also poses a problem for the conventional cutter edge. Attempts are therefore being made to precision cast it for turbide blades but rejection rates have proved large owing to unsatisfactory surface finish and dimensional inaccuracies. There exists the possibility of casting these forms slightly over-size followed by E.C.M.

Fig. 8 gives the machining rate curve for three electrolytes and these can be seen to be linear. A current density of 190 amps/sq.in. was obtained

despite the presence of Niobium (1.5% - 2.5%) which tends to be readily oxidised.

It is to be regretted that surface finish values were high, see Figure 15, being of the order of 140-170µ-inch. This surface was pitted and on close examination grain needles were clearly defined. Under the conditions of the tests made final finishing by E.C.M. would not be satisfactory but it is believed that the presence of niobium is partially responsible and further investigation may prove beneficial.

Henry Wiggins Nimonic 115

This is one of the most advanced nimonic materials produced to date. It differs from Nimonic 110 in that it contains neither aluminium, iron, silicon, manganese, boron nor zirconium. Its application is vital to the aircraft industry for first and second stage turbine rotor-blades.

Figure 9 indicates maximum removal rates possible within the limitations of the available power supply. Machining at current density values of 70 amps/sq. inch and 100 amps/sq. inch (namely 250 amp and 350 amps supply respectively) caused the surface of workpiece to have a thin grey/green film of acid when using each electrolyte. A gap of .008 inch was satisfactory at these values and facilitated continuous machining conditions. It was necessary, however, to increase the gap to .010 inch at 110 amps/sq.inch and 125 amps/sq. inch (400 amps and 450 amps supply respectively). At the .008 inch setting build-up of a surface layer on both anode and cathode tended to persist and would necessitate regular shut-down.

Fig. 15 shows that the surface finish of 15µ-inch obtained is superior to any other of the alloys examined and is not substantially affected by current density values.

Material - Titanium Hylite 50

The physical properties of titanium are by now well appreciated within the aircraft industry, and uses for this metal in situations in which both material lightness and strength properties are an important criteria, are becoming numerous. This particular titanium alloy is being used for making large area form-type blade aerofoils, both stator and rotor, by Bristol Siddeley Engines Limited. The present method of manufacture is to either finish machine the blade from a suitable casting or to machine the blade complete from a solid alloy blank.

It can be appreciated that the instantaneous formation of the protective oxide film on the surface of titanium makes it a difficult material to work, particularly electro-chemically, and it is of interest to note here that the repair or growth of the protective oxide film in a wide range of media can be stimulated by connecting the titanium to a positive source of

direct current. In this way titanium becomes a suitable medium to use in environments containing highly corrosive chemicals. It was not surprising therefore, to find that this particular specimen proved difficult to machine electro-chemically. Owing to the future importance of its application the procedure of investigation is covered in detail.

Specimen preparation for initial machining attempts included a final grinding operation to obtain the required size for locating purposes. Good contact between the material and the positive current electrode was then ensured by the firm fixing of a copper plate onto the specimen with screws and tapped locations. The exposed surface was thoroughly abraded mechanically and an attempt made to pass current. The electrolyte type used at this stage was 10.5% NaCl. All efforts to pass a current greater than 50 amps at 14.5 volts potential, were unsuccessful despite further surface cleaning.

Electrolyte strength was increased to 15.5% NaCl solution and more attempts made to break through the oxide surface, but still without success.

The possibility of reverse-polarity machining was then investigated. It has the known ability to break-up the oxide film that is present on such materials as aluminium, copper and magnesium and is used as a technique when welding these materials. Several theories have been advanced to explain this cleaning action. One of these is based upon the effects of ionic bombardment. The electrons are considered to proceed from the work-piece to the anode simultaneously as positively charged ions are attracted to the workpiece surface. These ions strike the surface with great force, and the oxide layer is consequently broken up. A cleaning action is thus produced in a very similar manner to that of a sand blast operation. A second probable theory suggests that it is solely the action of the electrons leaving the surface which leads to oxide breakdown.

In order to put this technique to test on the Metkem Shaper the supply terminals were reversed, the electrolyte flow reduced slightly, and the specimen inserted in the unclean condition. Current was passed successfully, and build-up to 450 amps, representing 119 amps/sq. inch current density, was instantaneous. This action was maintained for thirty seconds at .010 inches gap.

Quick polarity reversal was then effected and the workpiece again became the anode. In this state initial current rise to 100 amps was instantaneous; the value then rose slowly to 450 amps. at a constant 12 volts E.M.F. Electrolyte flow was returned to maximum available. The specimen was then removed, quickly cleaned, weighed, and returned to the machining area. Positive polarity was maintained and the current values rose rapidly to 400 amps, again at 12 volts E.M.F. The specimen was machined for one minute at a .008 inches gap, removed, quickly weighed, abraded slightly, returned to the working area and again machined successfully, at 350 amps.

This was repeated at the 250 amps. and 200 amps. current values. Figure 10 gives the resulting removal rates for these tests. It was noted that during the test at 400 amps, current values were unsteady and fluctuations of up to 5 amps. occurred. This characteristic is a result of 'Periodicity' which is an indication that anode passivity is iminent. This phenomenon, which occurs at intermediate current densities can arise in several ways, and the following general explanation is offered in ref. 1:-

'During the initial period of active corrosion, a layer of concentrated metallic salt solution accumulates at the anodic surface, whilst the migration of hydrogen ions towards the cathode leaves the liquid next to the anode less acid; these factors combine to produce passivity'. (i.e. anode passivity is more readily induced in an alkali salt environment).

'As soon as passivity arises, the discharge of hydroxyl ions again renders the solution more acid, whilst the evolution of oxygen stirs up the solution, dispelling the concentrated layer and thus restoring conditions favourable to active attack on the anode. When activity returns, the changes once more begin to operate in favour of the passive state, and in this way arise the fluctuations between activity and passivity; the frequency of the alterations depends on the nature of metal and solution, the current density and other conditions'.

It is suggested therefore that at the conditions of gap and flow considered the 400 amp current value, giving approximately 105 amps/sq. inch current density was approaching the machining rate limit for this material.

Further tests on this material were suspended for a period of several weeks whilst other investigations proceeded. During this time it was anticipated that a substantial surface oxide layer would be re-established and on resumption of testing this appeared to have happened. Initially the surface skin was lightly abraded using rough emery cloth and machining attempted under positive polarity conditions. Current did not rise above 100 amps. The surface was again cleaned and polarity reversed for twenty-five seconds. Machining was then relatively successful and current build-up to a maximum of 300 amps. was instantaneous. Current and electrolyte flow were cut, and on starting once more current build-up attained a maximum of only 130 amps. over a period of 30 seconds.

The specimen was then removed for further cleaning, quickly returned and current build-up time to a maximum of 300 amps. took 50 seconds. On removal the finish was particularly notable for its very rough dried-paint texture; and it appeared that attack had been mainly confined to grain boundaries.

The surface was thoroughly cleaned mechanically and on replacement, current build-up was instantaneous to 420 amps. at an E.M.F. of 13.5 volts. Slight current fluctuations were again evident at this value.

A test which entailed the stopping of current supply for thirty seconds with electrolyte still flowing, was conducted to assess the effect of an environment having no free oxygen content. On re-applying current supply, build-up to a maximum of 400 amps. was instantaneous, indicating that oxidation had not taken place. Following this, both current and electrolyte flow were stopped for two minutes and when re-established build-up to the same maximum of 400 amps. took approximately 8 seconds, indicating that slight oxidation had taken place. Surface finish readings measured using the Taylor Talysurf at .3 wavelength cut-off gave an average value of 155 μ-inch.

In conclusion the following points become apparent from the investigations:-

a) Reverse polarity machining will always ensure that the most tenacious of oxide films is broken down to enable this material to be corroded successfully.

b) Once the initial surface oxide build-up has been removed, successful machining characteristics can be achieved following mechanical surface abrasion.

c) The maximum surface current density values recommended for machining at electrolyte flow rates of 2500 gallons/hour, .010 inches working gap, approximate to 105 amps./sq. inch if anode passivity is to be prevented.

d) Titanium Hylite 50 may be machined satisfactorily at the above conditions using 15.5% strength NaCl electrolyte solution.

e) If the necessity to check gap width arises during a machining operation it is suggested that electrolyte flow is maintained to prevent surface oxidation and so facilitate the maintenance of satisfactory machining on re-application of current supply.

f) As limiting current density values are reached the phenomenon of 'periodicity' becomes noticeable.

g) Surface finish values are high at the current density values used during the investigation. They would not be generally acceptable for final finish.

Material K.E.805

This is one of a group of nickel, chromium, molybdenum steels which represent a link with the structural steels. Through having a low carbon content (0.3% - 0.6%) they are not capable of developing the high hardness or anti-abrasive resistance of other tool steels, but they possess considerably greater toughness. They are, therefore, ideally suited for small ruling sections of dies where applications involve severe vibration and repetitive loading.

The heat treatment applied to this alloy was as follows:

Oil quenched from 830°C
Tempered at 200°C

Figure 11 illustrates the machining rates for this alloy using the three electrolytes. It is interesting to note that when using the 15.5% Na Cl solution a dense oxide layer was obtained at 250 amps whilst at 450 amps the surface was clean although the machining rate had begun to fall-off. With other solutions the oxide layer persisted but was less substantial and the machining rate was unaffected.

Surface finish improved considerably with increase in current density. Figure 15 records a value of 29μ-inch at 120 amps/sq.in.

Material K.E.637

This oil-hardening steel contains approximately 0.8% - 1.0% carbon and 1.0% - 2% manganese. Owing to low martensitic transformation temperatures and consequent high austenite retention properties these steel types expand only slightly when hardened. They can nevertheless be hardened to values of 800 D.P.N. from a temperature of approximately 800°C. Distortion is minimised particularly if tempering temperature is low and these steels may therefore be heat treated after machining without noticeable dimensional inaccuracies becoming apparent. The toughness properties of this type of steel are high and their resistance to wear is good, particularly in conditions of shock loading.

The heat treatment for this material was as follows:-

Oil Quenched from 760 - 780°C
Tempered at 200°C.

Figure 16 gives the machining characteristics of this material. It is notable that the build-up of the oxide layer occurs later when using the nitrate salt and that anode passivity takes effect at a more rapid rate, once commenced, when using the least concentrated solution. This is unexpected, and although a ready explanation is not apparent, possible causes to consider are those of oxide porosity, or electrolyte temperature. (With respect to the latter the reader is referred to page 18 of this report).

The rapid build-up of an oxide layer was very noticeable at all the current density values used and efficiency is affected in all cases at densities above 90 amps/sq.in. However, as illustrated in Fig. 12, the sodium nitrate electrolyte offers advantages over the chloride solutions. The surface finish appeared 'speckled'. Talysurf readings were poor and affected but little by current density changes - see Fig. 15.

Material K.E.970

This alloy is a member of the high carbon, high chromium group. In the heat treated condition its structure consists mainly of a dispersion of hard chromium carbide in saturated martensite, and it thus possesses a high degree of wear resistance. As the chromium content is high the metal possesses a degree of corrosion resistance only slightly inferior to that of the true martensitic stainless steels. Owing to its high carbon content its resistance to shock loading and vibration is low. Industrial applications therefore are limited to pressing operations. Economics favour this material, however, for it is cheap and durable.

Figure 13 shows the machining characteristics. After each test the specimen surface was covered with a fairly adhesive brown oxide film. Difficulty was encountered in preventing metallic build-up in places on the surface when machining at the higher current densities. Gap width had to be increased to counteract this.

Surface finish values are given in Figure 15. Although some improvement is to be gained with increase in current density they remain very high.

General conclusions

The characteristics of the high strength, high temperature property materials applicable to aero engine use, namely the nickel based nimonics, the iron based P.E.11, the cobalt based Deloro X-40 indicate that they can be finish machined to satisfactory surface finish requirements when using the electrolyte/current density combinations investigated.

Although the oxide film experienced with F.V.448 did not detrimentally affect the machining rate it is possible that it caused the poorer surface finish. Should an improvement be desirable further research with other electrolytes may reveal benefits.

The nickel based alloy G.64 machined with extremely poor surface finish values and in this respect the technique offers no advantage over conventional methods. It is doubtful that any worthwhile advantage could be gained from the use of other electrolytes.

The ready formation of an oxide layer when machining the die steel specimens gives cause for concern, especially with K.E.637 and K.E.970. Higher electrolyte flow rates may be beneficial but this could lead to difficulties for large surface area installations. Again further research with other electrolytes may reveal advantages. Machining K.E.805 gives a good surface finish but only if current density is high.

Preferential grain boundary attack was not noticeable under the conditions considered.

Titanium presents a difficult machining problem which nevertheless can be effectively overcome by the application of the current reversal techniques formulated during this investigation.

Electrolyte heating effects

There are two distinct sources of heat input to the electrolyte:-

1) Kinetic energy transmitted to the fluid.
2) Electrical energy across the working gap.

The combined effect of these heat sources is to raise electrolyte temperature at rates with which normal environmental cooling cannot compete. However, the resistance of the electrolyte will be lowered at higher temperatures, so raising ionic mobility rates to give increased machining efficiency. A compromise must be made, therefore, between those conditions dictating an upper temperature limit and those requiring higher values.

During investigations it was found that at about 50°C the effect on the Perspex container created rather irratic cathode movement and the flexible P.V.C. conduit pipe expanded visibly under the fluid pressure generated. Therefore the maximum continuous temperature should be limited to, say, 45°C.

The heat input due to mechanical pump sources alone was evaluated by running the machine without current supply. The working gap was set at .008 inch with flow rate at its maximum of 2,500 gallons per hour. Temperature was noted at intervals for one hour and a half and results recorded in Fig. 18 curve (ii).

The heat input due to combined electric and mechanical sources was evaluated under working conditions using mild steel as a work material. The same gap and flow conditions were made to prevail and current was maintained constant at 400 amps by dropping the potential from 5.0 to 4.5 volts as the electrolyte resistance dropped. Temperature was noted at intervals for one hour and results are recorded in Fig. 18 Curve (i).

Lack of time prevented further investigation of other parameters such as different starting temperatures, different working gaps, different flow rates and different current values but the conditions examined are typical and the results can be used to estimate the allowable working time without a cooling system. Should a cooling system be incorporated under the same working conditions using 20 gallons of electrolyte it would have to be capable of cooling at the rate of 0.2°C per minute. General machining efficiency would be enhanced by incorporating a separate source of heat to raise the electrolyte temperature to 45°C before machining and to maintain it at that temperature between operating cycles.

Note that an increase in gap size requires an increase in electrical power to maintain the same current value, see Figs. 19, 20 and 21. Hence I^2R heating will increase approximately proportionally to gap size. However, for a constant electrolyte volume flow rate the hydrodynamic heating will decrease with increase in gap size. It may be possible,

therefore, to obtain optimum conditions for minimum rate of temperature rise but much will depend on the maximum power output from both electrical and pump supplies.

Physical surface effects

The state of stress existing at the surface layer of a component has often to be considered when determining optimum conditions in service, especially if the operating system is one in which fatigue properties are important. Residual compressive surface stresses generally improve component life when operating under tensile service. Under the same service, residual tensile surface stresses and/or poor surface finishes generally reduce component life. Surface finish has been reported earlier and the following limited investigation was carried out to determine the surface stress effects of E.C.M.

The need to have specimens initially stress-free can be appreciated. After machining 14 swg mild steel to dimensions suited to the Hounsfield Tensometer the specimens were stretched into the plastic range so that on springback they were stress-free and flat. Each specimen was 0.5 inch wide and after stretching fell between 0.0720 and 0.0725 inch. in thickness. A section 2.03 inch in length was cut from each piece and lightly filed to a final length of 2.00 inch.

The initial radius of curvature was measured over a 1.500 inch gauge length using the equipment shown in Fig. 22. This comprises an accurate three-point positioning jig, an end locating screw and a small ball-ended inductive transducer mounted to contact each specimen at mid-gauge length. The transducer forms part of Magnagauge equipment which, as a centre-reading device, has a full deflection reading of ± .0005 inch with each .0001 division sub-divided into .00001 inch.

A special fixture had to be used to hold the specimen during E.C.M. and because of this gap size could not be less than .050. Current density was maintained at 115 amps/sq.inch and electrolyte flow at its maximum to reduce the specimen thickness from .0720 to .0390 inch. This was carried out in steps to permit periodic removal for deflection measurement.

For comparison, two specimens were machined on a conventional surface grinder set to remove .001 inch per pass. Deflection readings were taken during a .016 reduction in thickness.

Results are tabulated below and graphically illustrated in Fig. 23.

Process	Thickness	Deflection from zero	Cumulative change in deflection	Surface Finish
1) E.C.M.	.0720(orig)	-.00005	0	
	.0680	-.00005	0	
	.0610	-.00005	-0.00005	
	.0510	-.0001	-0.00005	
	.0390	-.0003	-0.00025	8μ"
2) Grind	.0720(orig)	+.00048	0	
	.0650	+.00030	-0.00018	
	.0635	+.00010	-0.00038	
	.0560	-.0006(approx.)	-0.001	17μ"
3) Grind	.0725(orig)	-.00055	0	
	.0670	-.00012	+0.00043	
	.0560	+.0003	+0.00085	20μ"

Deflection over 1.5 inch gauge length during machining

The change in curvature during E.C.M. is extremely small. For the first .011 inch machined no change was measured, indicating that surface stresses were not being induced. The only alternative to this conclusion would be that the induced stress system balanced the stress system removed; this is highly improbable. On removing a further .022 inch a slight change was measured and it is suggested that this is due entirely to the removal of stressed layers even though the specimen had been stretched. This change is very small compared with the results obtained from the grinding process which is well-known for its stress inducing characteristics.

The investigation of relative cathode-anode shape

The final profile of an anode workpiece is never an exact replica of the cathode former. Generally the more pronounced the initial profile difference between the two, the greater is the difference in final form. Forevery finished anode profile, however, there must be a former of a certain shape which will produce the dimensions required. This is called the 'Electrolytic Shape' of the cathode, and it is the difficulty of obtaining this shape which is responsible for a large proportion of the long pre-production planning times necessary in industry.

Present electrode shaping methods are trial and error techniques, involving the gradual addition and removal of metal, as required, from the former surface. Rolls-Royce use a technique for obtaining their cathode formers for blade production, whereby the final product form is machined accurately out of either copper or stainless steel, using conventional machining methods. This specimen becomes a male cathode; a suitable workpiece material, (mild steel) is chosen and the resultant shape is machined into this electro-chemically. By taking a plaster mould of the shape of this anode, its form can be accurately reproduced by profile machining, and the final cathode shape thus manufactured. Trial runs are made using this shape, necessary modifications are made, as and where required, to give the precise form needed.

This is the most satisfactory method evolved to date but, although quite rapid and readily adaptable, will have limitations for die sinking and other accurate forming over deep sections.

In what follows the authors have made no attempt to evolve a rigorous solution for the prediction of cathode shapes. The experiments were conducted to introduce the investigators to the parameters involved and so form a foundation for future work.

The investigation was divided into two parts; examination of static potential fields and dynamic tests using the Metkem Shaper.

The equipment for the field plotting examination is shown in Fig. 24 and 25 and comprises an A.C. Bridge unit, a Newall Jig Boring machine (used only because of the suitability of its co-ordinate table and spindle) and equipment for direct recording of the field distribution onto paper.

The A.C. Bridge Unit - Fig. 26 incorporates a 50 c/s 9 volt supply to a potentiometer R1 to R10 and to the electrodes. The potential across the tapping point and detector probe is rectified by the synchronous switch VT1. Diodes D1 and D2 serve to protect the centre-zero meter M1 by reducing the sensitivity when the potential difference is large. It is quite safe even if the probe contacts an electrode. Should the electrodes inadvertently be made to contact each other the warning lamp LP2 lights and remedial action can be taken to protect the transformer. Since neither probe nor electrodes are earthed the bridge unit and tank must rest on insulated surfaces.

If the electrodes are not of similar material a D.C. potential is generated which upsets the zero setting. This was witnessed when using brass electrodes and a .015 inch diameter probe manufacturel from a high speed steel drill. However, this effect can be calibrated and correction factors applied to the Ml reading.

The slideways of the Newall jig-borer facilitate smooth movement and accurate positioning of tank and probe over the required range. The machine was accurately levelled to give uniform 0.5 inch depth of water in the perspex tank. A small amount of liquid soap was added to the water as a wetting agent and as an aid to conductivity.

Using a variety of fixed-state profiles the equi-potential distributions shown in Figs. 27 and 28 were obtained. (The relative positioning of anode and cathode electrodes was governed more by display requirements than by considerations of actual machining dimensions). The lines drawn normal to the electrode surfaces and the equi-potential lines represent ionic paths. Current density at any point on an electrode surface is inversely proportional to the coincident path length. Thus, the current distribution over the complete anode surface can be determined and will correspond to the distribution of metal removal rate.

To obtain close correlation with actual machining conditions, electrodes were manufactured to simulate the changing anode shapes then operating. The distance between electrodes was made proportional to those typically used in practice and as each plot was determined, the current distribution over the anode surface was calculated and the typical metal removal computed for a specific time interval. Successive corresponding profiles were then constructed e.g. Fig. 29 and 31 and further plots taken. The fields thus obtained are illustrated in Figs. 30 and 32.

The cathode electrodes used for the dynamic tests are shown in Figs. 33 and 34 together with the final forms machined in the mild steel anode specimens using 15% Na Cl electrolyte. Each specimen was made in the form of three laminated sections in order that the centre section, free from edge rounding effects, could be removed for profile measuring purposes. The mounting jig was designed to facilitate easy removal from the machine and assured accurate replacement.

Throughout the tests the minimum gap was maintained at .020 inch and the 15% Na Cl electrolyte was set at maximum flow rate. Specimens were split at regular intervals of 0.250 cathode displacement and the profile recorded by tracing the magnified image on an Isoma Projector.

Static field plots Fig. 27 illustrate the change in current distribution when an alteration of 40% is made in the minimum gap dimension. These verify the expectation of the following dynamic conditions:-

(i) A decrease in minimum gap creates a greater percentage intensity over that element so enabling faster initial feed rates to be achieved.

(ii) Final workpiece profile will be obtained more rapidly and with greater accuracy as the minimum gap is decreased.

The effect of minimum gap upon profile accuracy under dynamic conditions was obtained using a square former having .012 inch radius edges, see Fig. 33. The results are indicated by the curves of Fig. 36(a) and (b). A marked increase in the workpiece corner radius occurs for gap sizes greater than .010 inch but very little improvement is obtained below this figure. By extrapolation to .002 inch gap the corner radius would fall only to .039 inch (325% electrode radius) from that of .043 inch (361% electrode radius).

The dynamic test results shown in Fig. 35 can be compared with the static prediction of Fig. 29 to indicate the extent to which agreement was obtained over the first 0.100 inch of penetration.

Fig. 28(a) shows the static current distribution between a flat anode and semi-circular cathode. Under dynamic conditions the recess machined in the anode would be of parabolic shape with a certain amount of edge fringing. Fig. 38(a) represents the ideal stages required during machining of a semi-circular recess; typical ionic paths are superimposed. The corresponding total charge distribution is parabolic, see Fig. 38(b).

The elliptic-shaped electrode used in the static examinations, Fig. 32, was used as a basis for design of the copper cathode shown in Fig. 34 for dynamic tests. Successive profiles obtained in a mild steel workpiece are shown in Fig. 37. The rounding of the edge of the recess was caused by the breakdown of the plastic masking agent placed on those parts of both anode and cathode from which the passage of current was not required. This breakdown was due entirely to the mechanical erosion of the flowing electrolyte and the suitability of non-conducting masking agents in this environment must be investigated before further dynamic shape examinations can proceed.

The step-by-step field analysis has proved quite a useful guide for design of the cathode profiles required under continuous machining conditions. However much remains to be investigated and analysed before absolute prediction can be achieved. Except for the most simple shapes, the many parameters to be considered hinder solutions of a rigorous, mathematical nature. Maximum efficiency in the utilisation of electrical power would only be obtained by maintaining a constant minimum gap since this ensures a minimum, cumulative path resistance. It would also assist shape prediction, and hence has been considered herein, but would normally require a programmed cathode feed rate to suit the changing profile conditions. Even if this programme was evolved, the necessary control system would add considerable cost to a machine. A feed control system based on the maintenance of constant current would guarantee a mean gap resistance, but may permit minimum gap to decrease to zero with consequent short circuiting. At present, the authors are of the opinion that a manually set, constant feed rate with an independant current supply capable of varying as the resistance of the gap demands has much in its favour and further work on shape prediction will be carried out on this basis.

Acknowledgements

The authors acknowledge with many thanks both The College of Aeronautics and Metachemical Machines Ltd. for providing the facilities which made possible the work reported herein. Thanks are especially due to Professor J. Loxham and his staff for their ready advice and assistance and similarly to staff in the Department of Materials and in the Instrumentation Section of the Department of Electrical and Control Engineering. Further thanks are due to Bristol Siddeley Engines Ltd., and Rolls-Royce Ltd. for the interest and hospitality shown during visits to their establishments.

References

1. Metallic Corrosion, Porosity and Protection 2nd Edition, Chapter V by U.R. Evans. Published by Arnold.

2. General and Inorganic Chemistry by P.J. Durrant. Published by Longmans.

3. Chemical Analysis of Metals and Alloys by Gregory and Stevenson. Published by Blackie.

4. Electro-Chemistry Vol. 1, 4th Edition, by Creighton and Cochler. Published by John Wiley and Sons.

5. Journal of Physical Chemistry 1908, p. 12-448.

6. Private communication from A. Hickling, University of Liverpool.

7. Unfamiliar Oxidation States and their Stabilisation, 1950, by Jacob Kleinberg, 1950, University of Kansas Press.

8. Steels and Modern Industry. Iliffe Press.

Appendix 1

Determination of removal rates based on Faraday's laws

E.C.E. of silver = .0011183 gms/coulomb

$$\text{E.C.E. of aluminium} = \frac{.0011183 \times \text{chemical eq. of } Al}{\text{chemical eq. of Ag}}$$

Chemical eq. of Ag = 107.88 (Valency 1)

$$\text{Chemical eq. of } Al = \frac{\text{Atomic weight}}{\text{Valency}} = \frac{26.97}{3}$$

$$\therefore \text{ E.C.E. of } Al = \frac{.0011183 \times 26.97}{3 \times 107.88}$$

$$= .00009319 \text{ gms/coulomb}$$

Example:

Consider a current of 250 amps flowing for 60 secs.

Total charge = 15,000 coulombs

Rate of aluminium removal = .00009319 x 15000

= 1.39785 grams/min.

= .031583 cu.ins./min.

If flat surface area = 3.175 x 1.25 sq.in.

Then cathode feed rate = .0080 ins/min.

Current amps.	Metal Removal Rate cu.ins/min.			Cathode feed ins/min.	
	Predicted	Actual	$\frac{\text{Actual}}{\text{Predicted}} \times 100\%$	Predicted	Actual
250	.0316	.0392	124	.0080	.012
300	.0379	.0452	119	.0096	.013
350	.0442	.0541	122	.0112	.016
400	.0505	.0630	125	.0128	.0175
450	.0568	.0710	125	.0144	.018
500	.0631	.0813	129	.0160	.021

The 'actual' rates above were obtained with 10.5% Na Cl electrolyte.

Appendix 2

Hydrogen generation whilst machining

Hydrogen is liberated by the dissociation of water through the electrolysis action. It is believed that the action is of the form:

$$2H_2O = OH_3^+ + OH^- \quad \ldots\ (1)$$

The hydroxonium ion OH_3^+ can be regarded as having been formed by the attachment of a hydrogen ion to a neutral water molecule. The active part of the ion which is of interest is H^+.

Consider the conventional action:

$$H_2O = H^+ + OH^- \quad \ldots\ (2)$$

That is, 1 gram-molecule of H_2O, which weighs 18 grams, will yield, on complete ionisation $\frac{1}{2}$ gram-molecule of hydrogen weighing 1 gram. Therefore, two gram-molecules of water will yield one gram-molecule of hydrogen occupying approx. 22 litres at S.T.P. 96,540 coulombs are required for this action.

Returning to reaction (1) above, then 2 x 96,540 coulombs will be required to generate 22 litres of hydrogen. At a current of 500 amps the rate of generation will be 3.4 litres per min. ($\simeq$ 200 cu.ins per min.) at S.T.P.

Appendix 3

Machining mild steel

At the anode, atoms, deprived of electrons go into solutions as cations. At low current density each atom looses two electrons, while, at high current density, three electrons. Thus ferrous and ferric ions are yielded respectively:

$Fe = Fe^{++}$ i.e. Ferrous

$Fe = Fe^{+++}$ i.e. Ferric.

The main anion in solution is Cl^-; consequently the anode machining product is $FeCl_2$ or $FeCl_3$. Both of these salts are freely soluble.

At the cathode, two reactions can occur, each leading to alkalinity. Lack of oxygen will lead to hydrogen evolution:

$$2H^+ + 2e = H_2$$

while, with oxygen, hydroxyl ions will be produced:

$$O_2 + 2H_2O + 4e = 4(OH)^-$$

Consequently, the cathodic product will be hydrogen or sodium hydroxide or a combination of both.

Between the two electrodes iron chloride and sodium hydroxide could interact to form the insoluble hydroxides of iron, while sodium chloride will be regenerated. The hydroxides will be responsible for the rapid discolouration of electrolyte which takes place during machining.

With ferric chloride the reaction would probably be

$$FeCl_3 + 3NaOH = FeO(OH) + 3NaCl + H_2O$$

where the brown ferric hydroxide is in the part-hydrated form, found normally as the chief constituent of iron rust. The brown precipitate which forms in the electrolyte would then be $Fe(OH_3)$:-

$$FeO(OH) + H_2O = Fe(OH)_3$$

With ferrous chloride the reaction would probably be

$$FeCl_2 + 2NaOH = Fe(OH)_2 + 2NaCl$$

and since the surface of the workpiece was light green at the low current densities there is some support for this.

Should sufficient oxygen be available at higher current densities the part-hydrated form of ferric hydroxide may again be formed:

$$4Fe(OH)_2 + O_2 = 4FeO(OH) + 2H_2O$$

and result in the brown precipitate $Fe(OH)_3$ as above.

If, however, oxygen supply is limited the magnetic oxide of iron may be formed:

$$6Fe(OH)_2 + O_2 = 2Fe_3O_4 + 6H_2O$$

support for which is gained by noting that at the higher current densities tested the surface of the workpiece became black.

The experiments reported herein did not include a chemical analysis of the workpiece surface layer nor of the precipitate in the electrolyte. The above possibilities are included to introduce the reader to the reactions which may occur. Fortunately, the electrolyte flow was sufficient to prevent passivity tendencies but these may arise at higher current densities than those tested and, if so, would cause a reduction in the machining rate in a similar manner to that experienced with aluminium.

Of possible interest to the reader is the fact that the pH of the electrolyte changed from a neutral value of 7 to between 6 and 6.5 over long periods of machining.

Figure 14 illustrates the removal rates obtained and superimposed are the expected rates for Ferrous Chloride and Ferric Chloride formation. These rates correspond to their electro-chemical equivalents:

.000289 gms/coulomb - Ferrous

.0001925 gms/coulomb - Ferric.

Appendix 4

Material specifications

P.E.11	Chromium	17% - 19%
	Molybdenum	4.75% - 5.75%
	Titanium	2.10% - 2.5%
	Aluminium and titanium	2.7% - 3.5%
	Nickel and cobalt	37% - 39%
	Others - Zirconium, Lead, Boron, Silicon, Manganese, Copper	
	Iron	The remainder.
X 40	Chromium	24.5% - 26.5%
	Nickel	9.0% - 12.5%
	Tungsten	7.0% - 8.0%
	Iron	2.0% -
	Mangarese	1.0%
	Silicon	1.0%
	Cobalt	50.0% - 55%
F.V.448	Chromium	10% - 12%
	Silicon	0.2% - 0.65%
	Carbon	0.08% - 0.15%
	Iron	The remainder.
G.64	Chromium	10% - 12%
	Niobium	1.5% - 2.5%
	Iron	5.0% -
	Aluminium	1.5% - 5.5%
	Molybdenum	2.0% - 4.0%
	Tungsten	2.0% - 5.0%
	Nickel	65% - 70%
Nimonic 115	Chromium	13% - 17%
	Cobalt	13% - 17%
	Titanium	3% - 5%
	Molybdenum	3% - 5%
	Nickel	The remainder

Titanium Hylite 50	Aluminium	3% - 5%
	Molybdenum	3% - 5%
	Tin	1.5% - 2.0%
	Silicon	0.3% - 0.7%
	Titanium	The remainder.

K.E.805 — High grade, electrically melted, direct oil hardening nickel, chrome, molybdenum steel.

K.E.637 — Low temperature, oil hardening alloy tool steel.

K.E.970 — High duty tool steel with 2% carbon, 14% chromium.

Index to figures

Fig.28(a) Static field and current distribution for semi-circular cathode and flat anode - max. current density at centre
Fig.28(b) Static field and current distribution for semi-circular cathode and anode - large gap
Fig.28(c) Static field and current distribution for semi-circular cathode and anode - small gap
Fig.28(d) Static field for square anode, sharp wedge cathode - note current concentration at square edges

---

Fig.29 Progressive anode shapes with rectangular cathode determined from static fields at discreet time intervals

---

Fig.30(a) Static field for rectangular cathode and flat anode

---

Fig.30(b) Progressive static fields with rectangular cathode

Fig.31 Simulated electrode shapes for static plots
Fig.32(a) Static field with elliptic cathode and flat anode

Fig.32(b) Progressive static fields with elliptic cathode

Fig.33 Two machining cathodes and typical workpiece
Fig.34 Elliptic cathode and workpiece before and after machining

---

Fig.35 Workpiece profiles during machining

Fig.36(a) Workpiece corner radius, minimum gap relationship with rectangular cathode having .012 edge radius
Fig.36(b) Per cent. workpiece corner radius to cathode radius with increasing gap

---

Fig.37 Workpiece profiles during machining with elliptic cathode
Fig.38(a) Ideal workpiece profiles required during machining

Fig.38(b) Current distribution required to obtain ideal profiles (a)

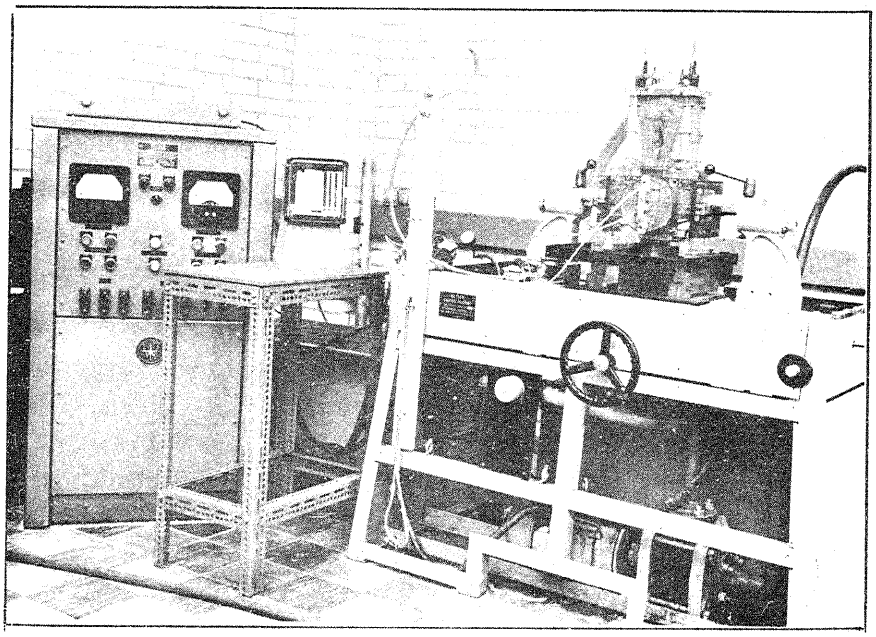

FIG. 1 THE METKEM SHAPER MACHINE

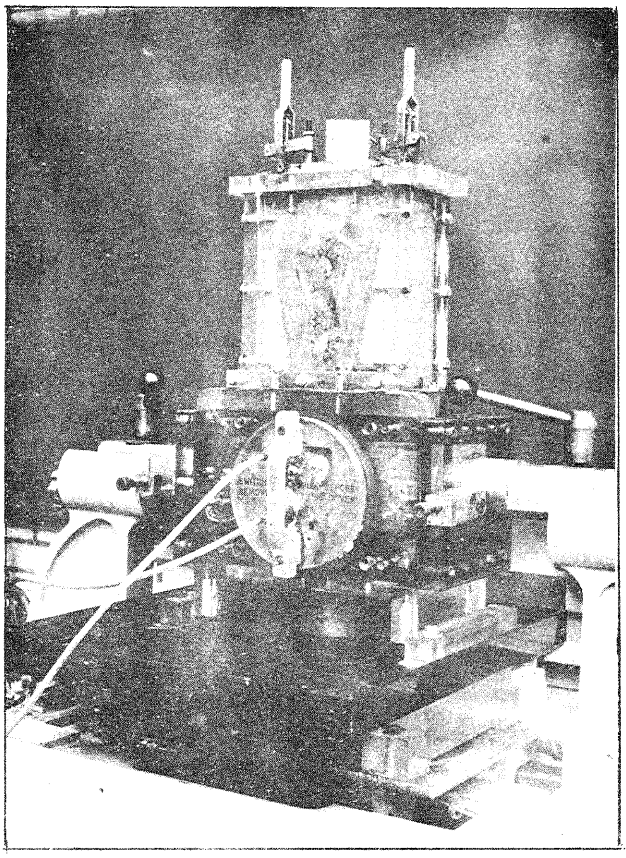

FIG. 2. THE WORKING AREA

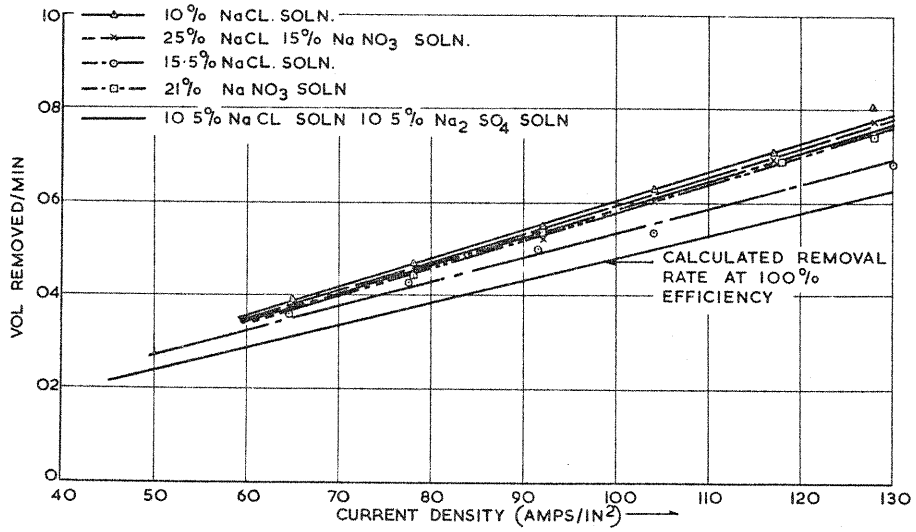

FIG. 3. MACHINING RATE FOR ALUMINIUM

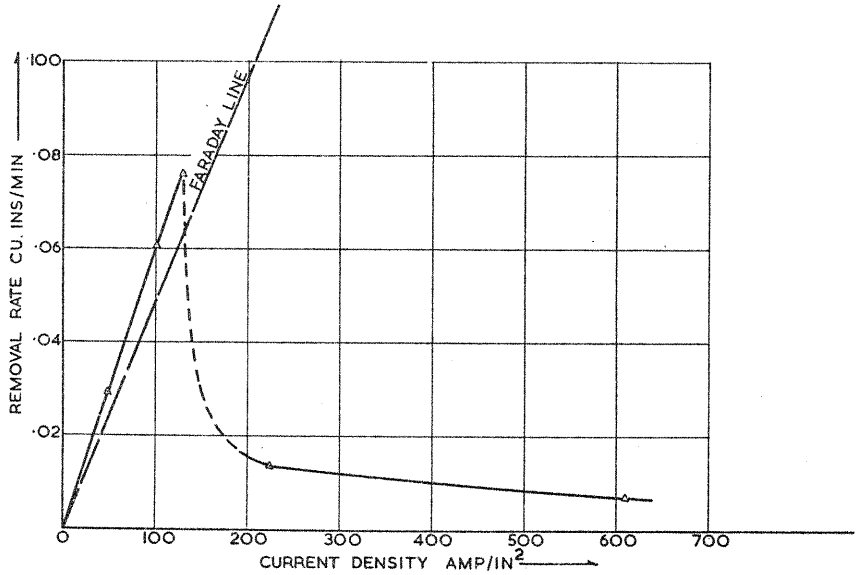

FIG. 4. MACHINING RATE LIMITATIONS FOR ALUMINIUM

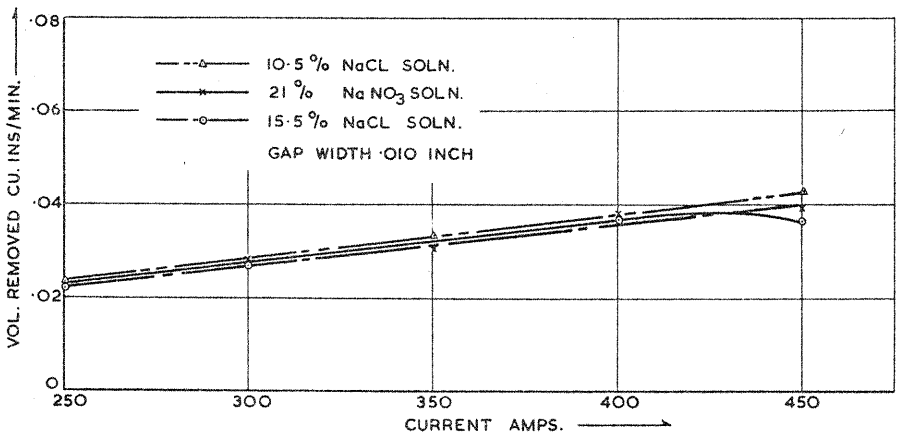

FIG. 5. MACHINING RATE FOR P.E.11.

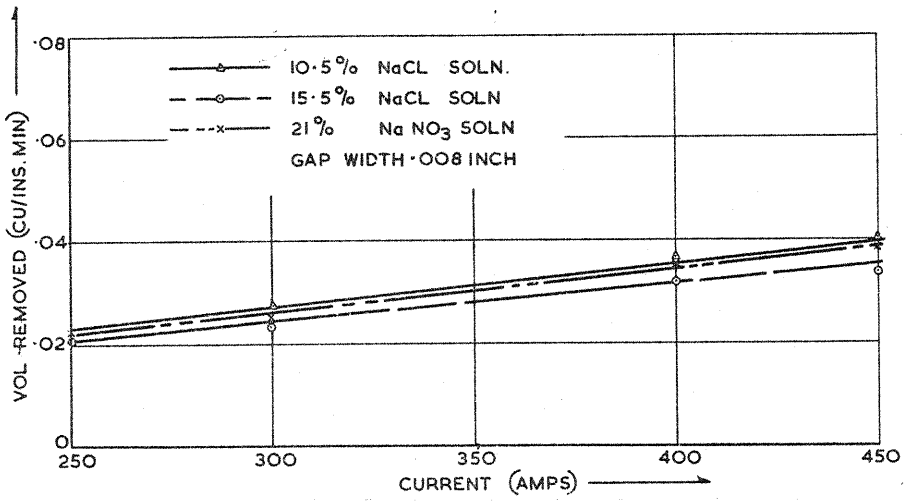

FIG. 6 MACHINING RATE FOR X.40

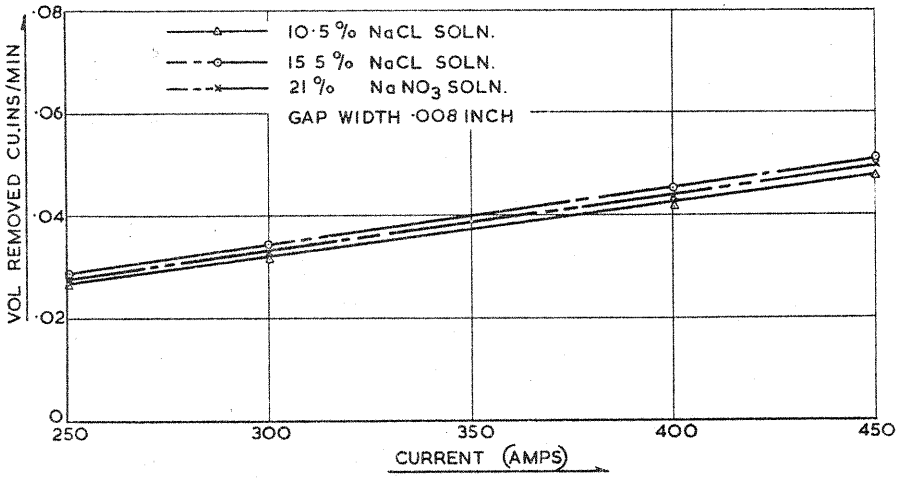

FIG. 7. MACHINING RATE FOR F.V.448

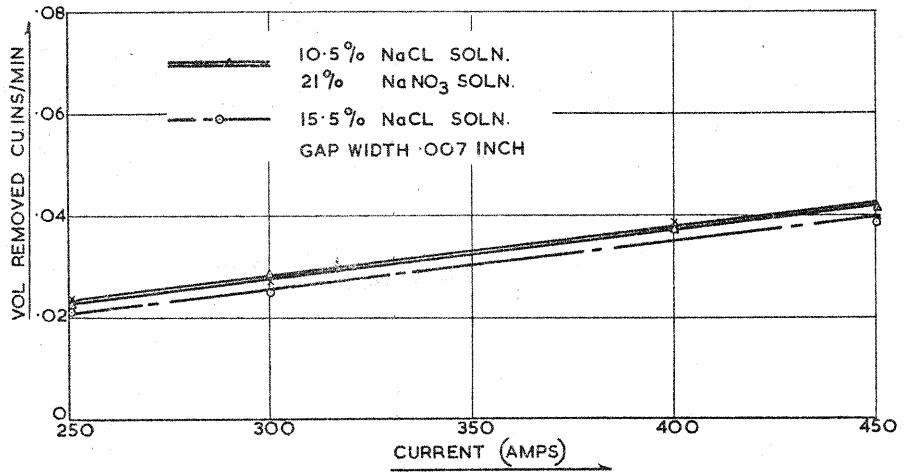

FIG. 8. MACHINING RATE FOR G.64

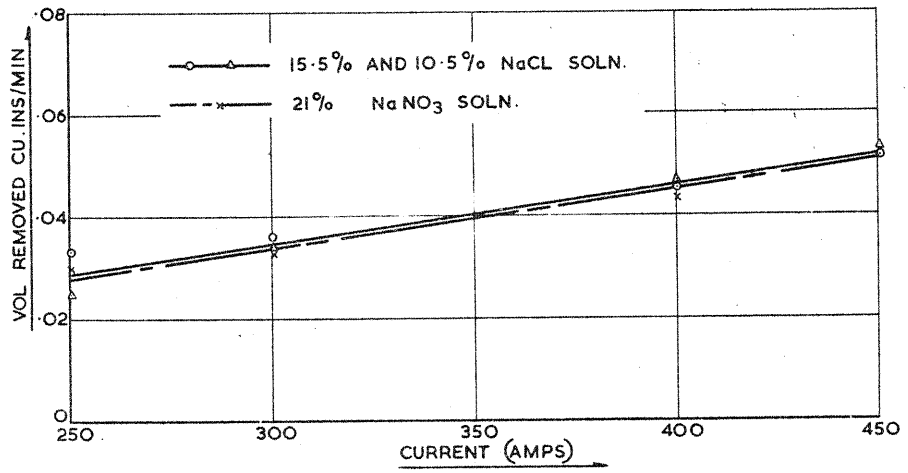

FIG. 9 MACHINING RATE FOR MIMONIC 115

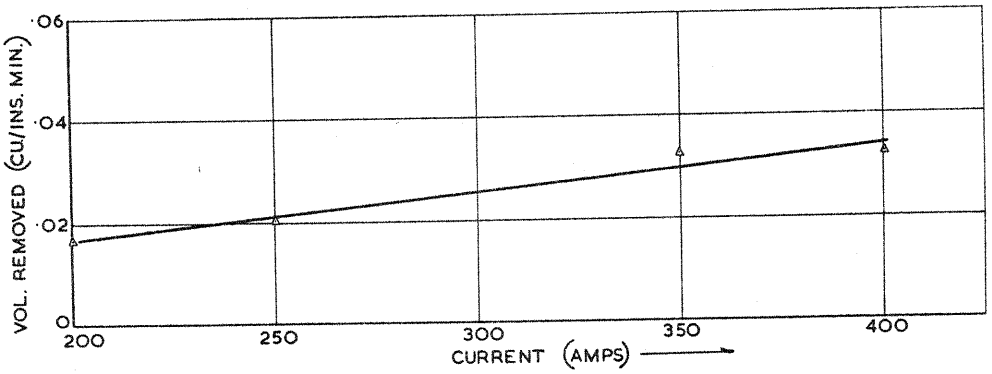

FIG. 10. MACHINING RATE FOR TITANIUM HYLITE 50 USING 15.5% NA C1 ELECTROLYTE.

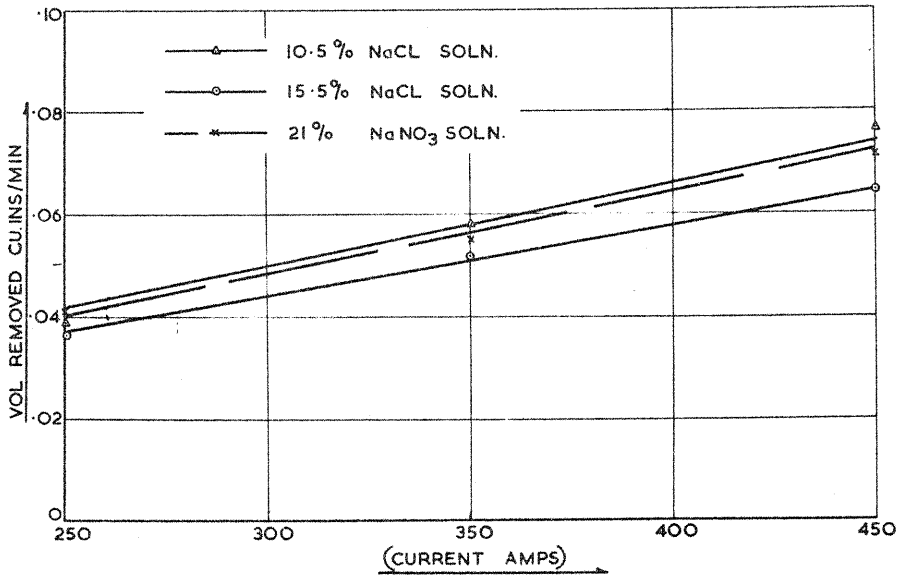

FIG. 11. MACHINING RATE FOR KE 805

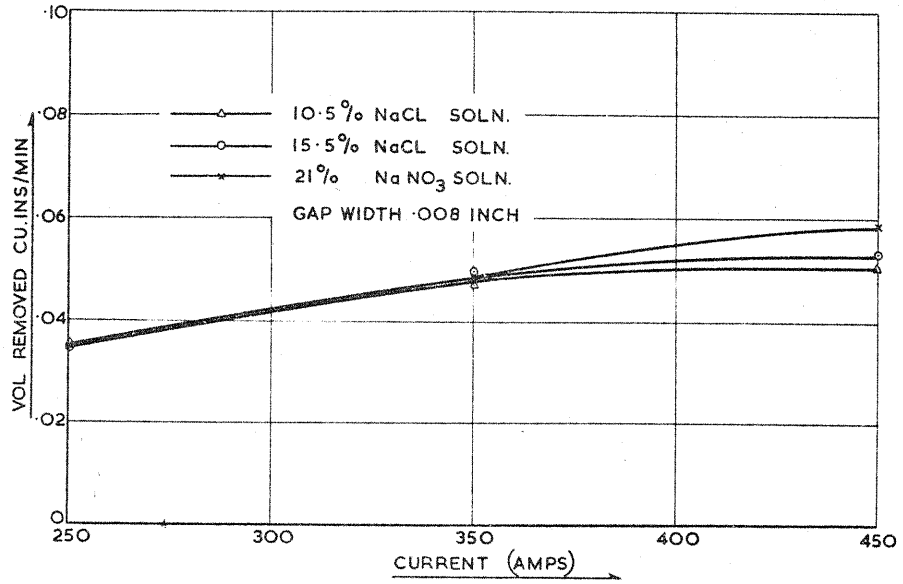

FIG. 12. MACHINING RATE FOR KE 637

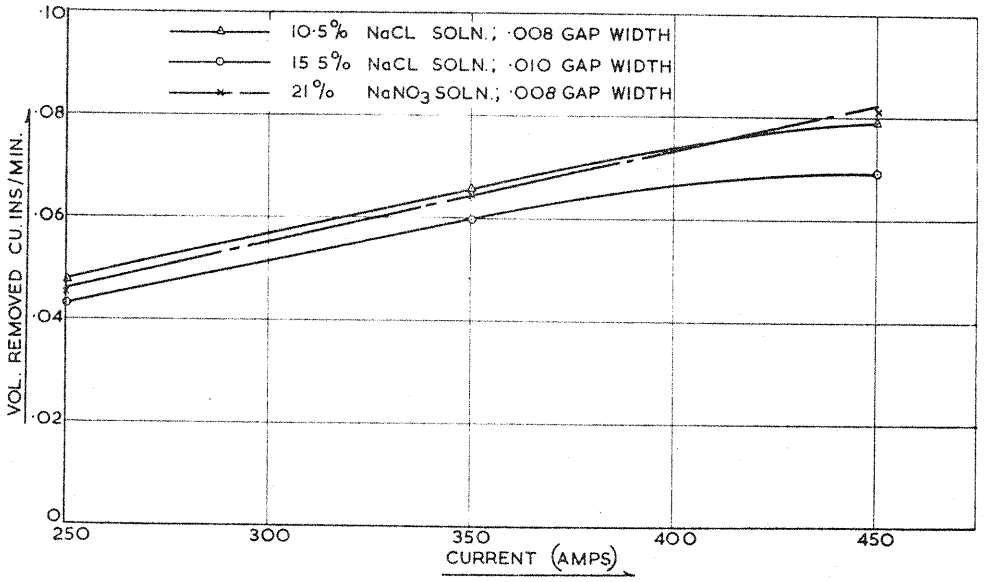

FIG. 13. MACHINING RATE FOR KE 970

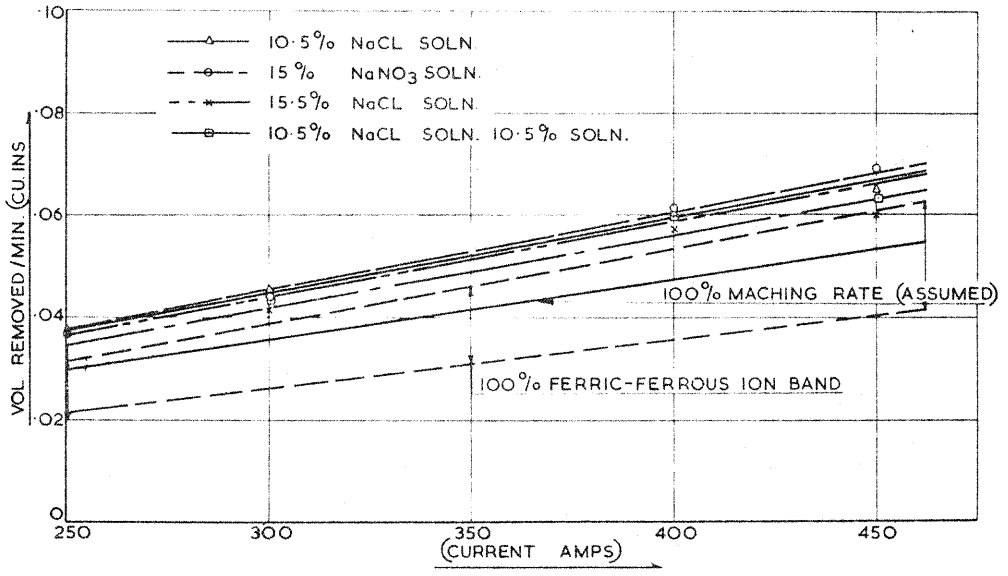

FIG. 14. MACHINING RATE FOR MILD STEEL

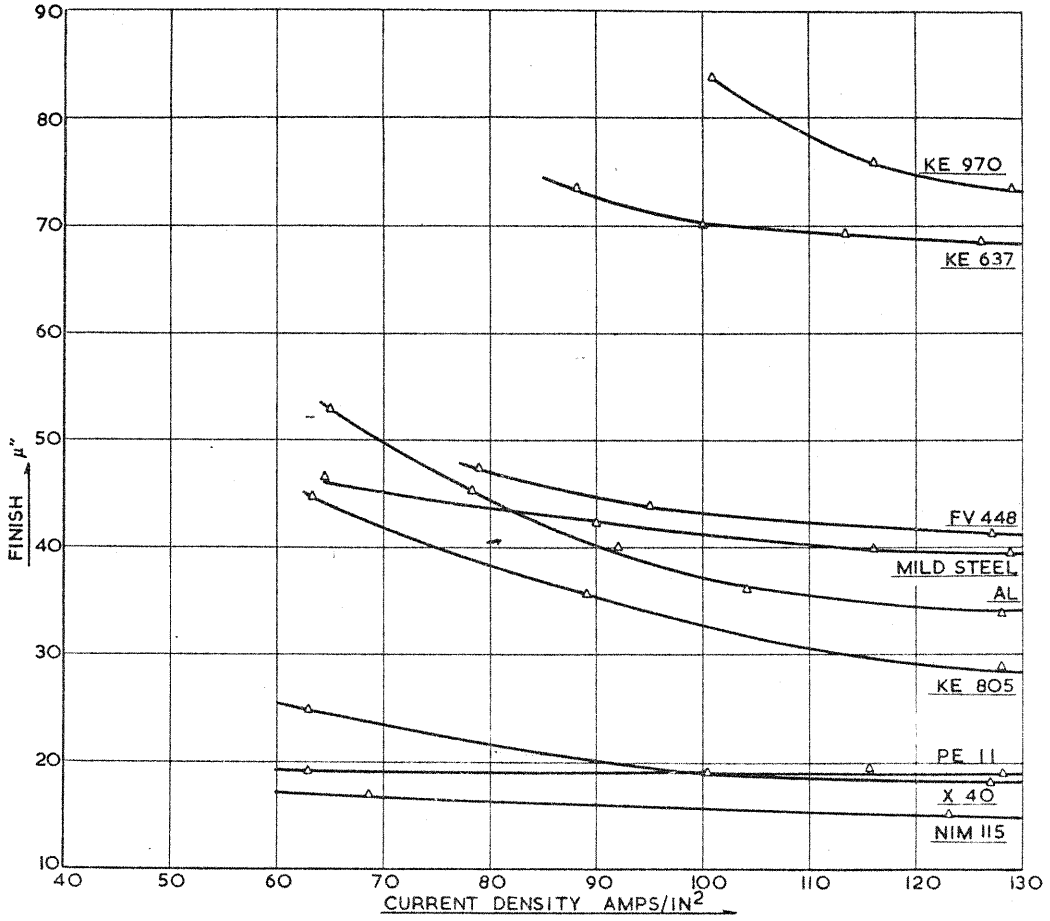

FIG. 15. SURFACE FINISH VALUES USING 15.5% NA C1 ELECTROLYTE

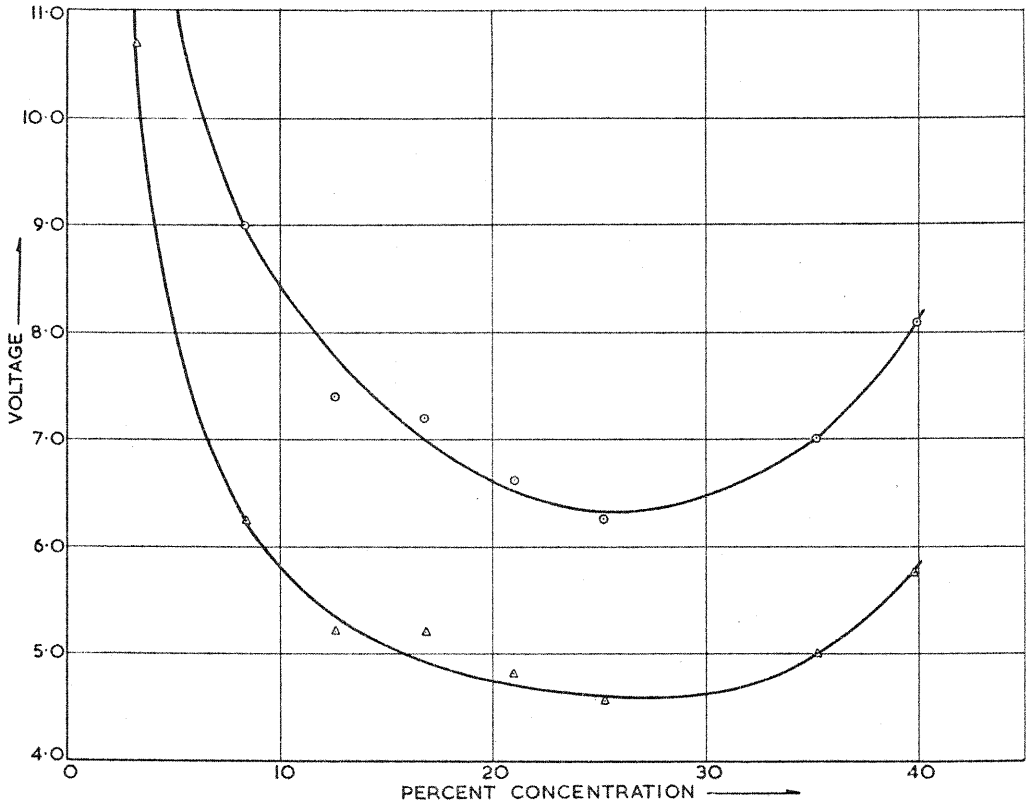

FIG. 16. VOLTAGE - ELECTROLYTE CONCENTRATION RELATIONSHIP AT CONSTANT CURRENT.

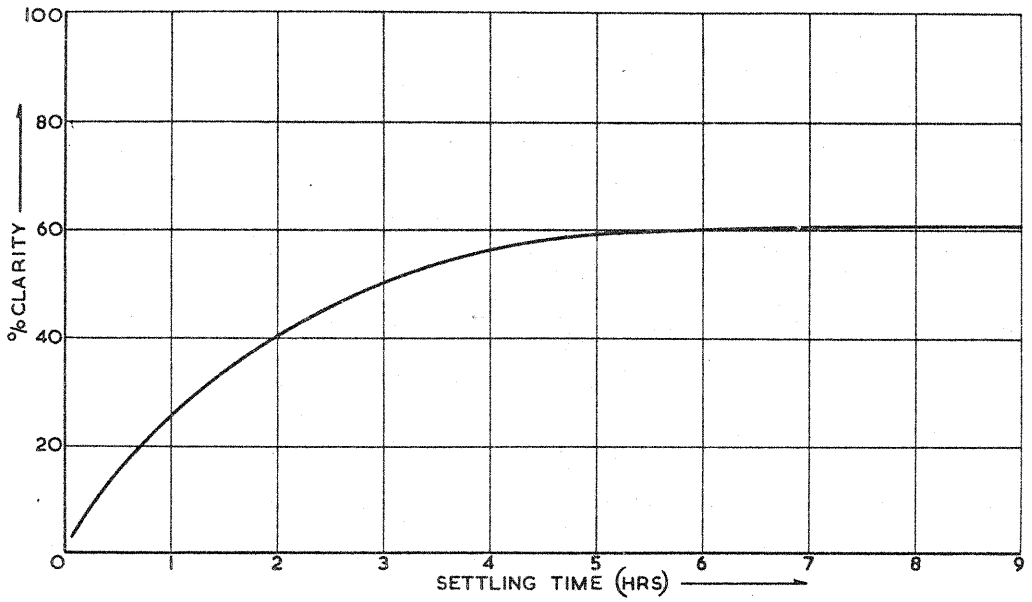

FIG. 17. PER. CENT CLARITY - SETTLING TIME RELATIONSHIP FOLLOWING THE MACHINING OF MILD STEEL WITH 10.5% NA C1 ELECTROLYTE.

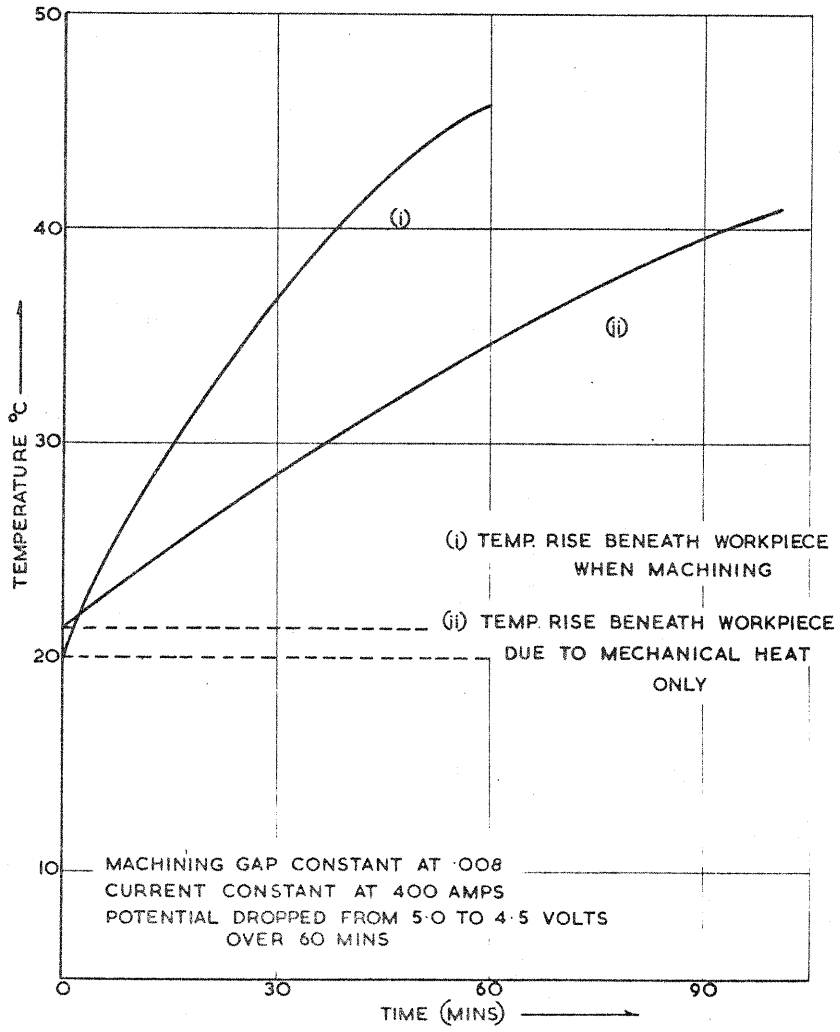

FIG. 18. ELECTROLYTE TEMPERATURE - WORKING TIME RELATIONSHIPS.

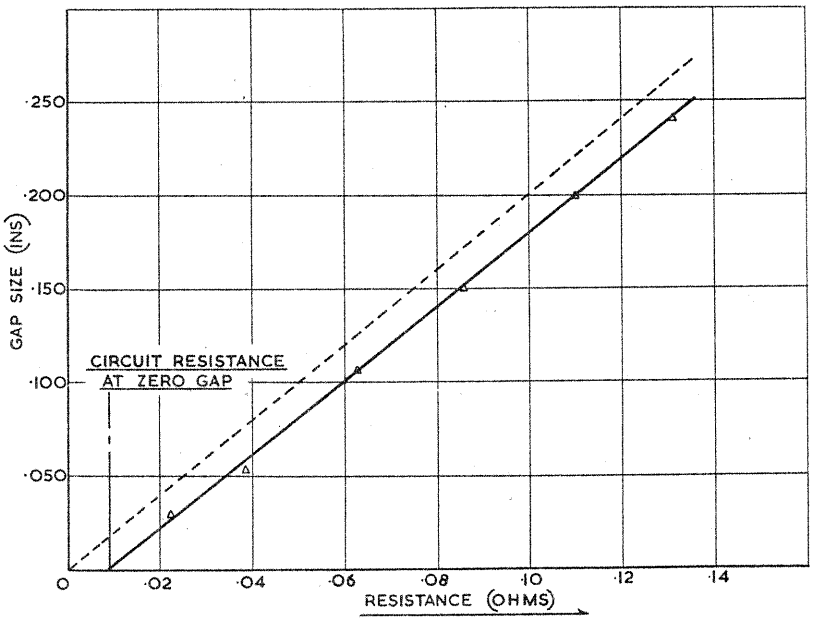

FIG. 19. TYPICAL GAP SIZE, ELECTRICAL RESISTANCE RELATIONSHIP FOR 10.5% NA C1 ELECTROLYTE

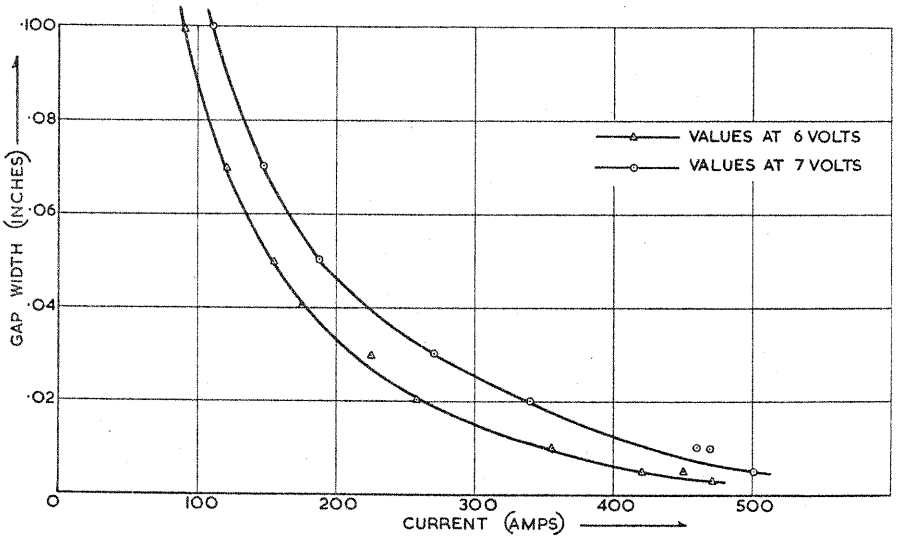

FIG. 20. GAP SIZE, CURRENT RELATIONSHIP AT CONSTANT VOLTAGE

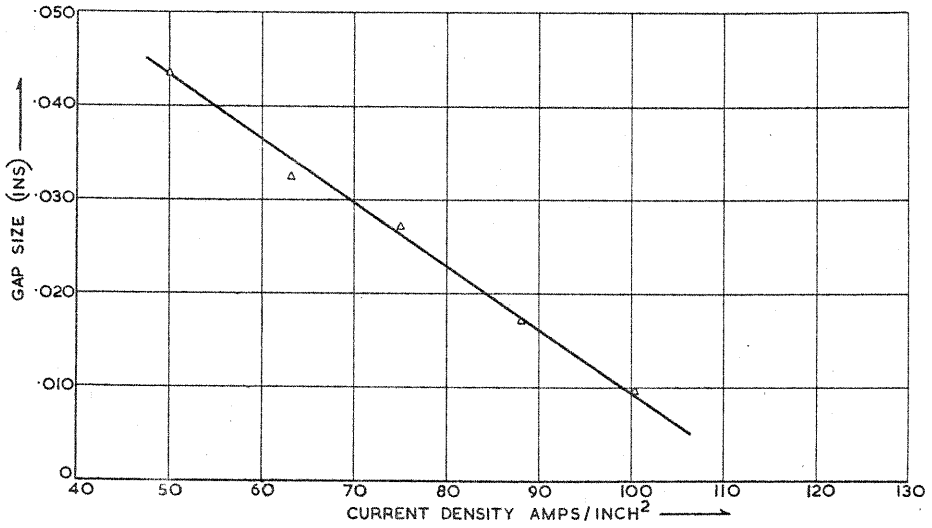

FIG. 21. GAP SIZE, CURRENT DENSITY RELATIONSHIP AT CONSTANT VOLTAGE (CURVE IS REASONABLY LINEAR OVER RANGE CONSIDERED)

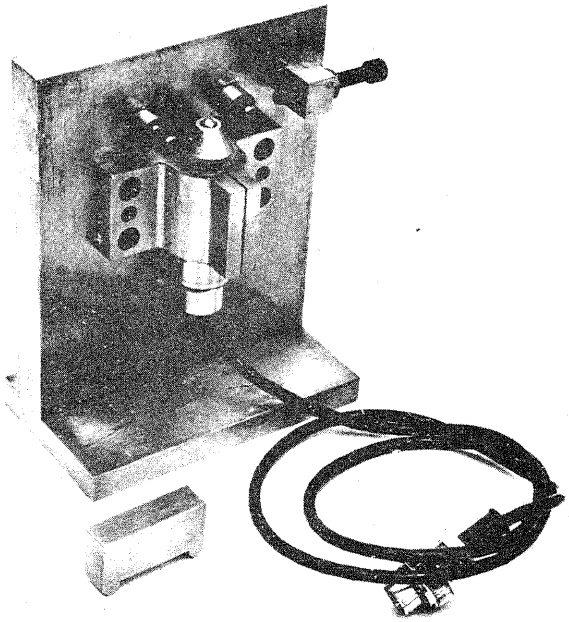

FIG. 22. CURVATURE MEASURING JIG WITH TRANSDUCER FOR MAGNAGUAGE

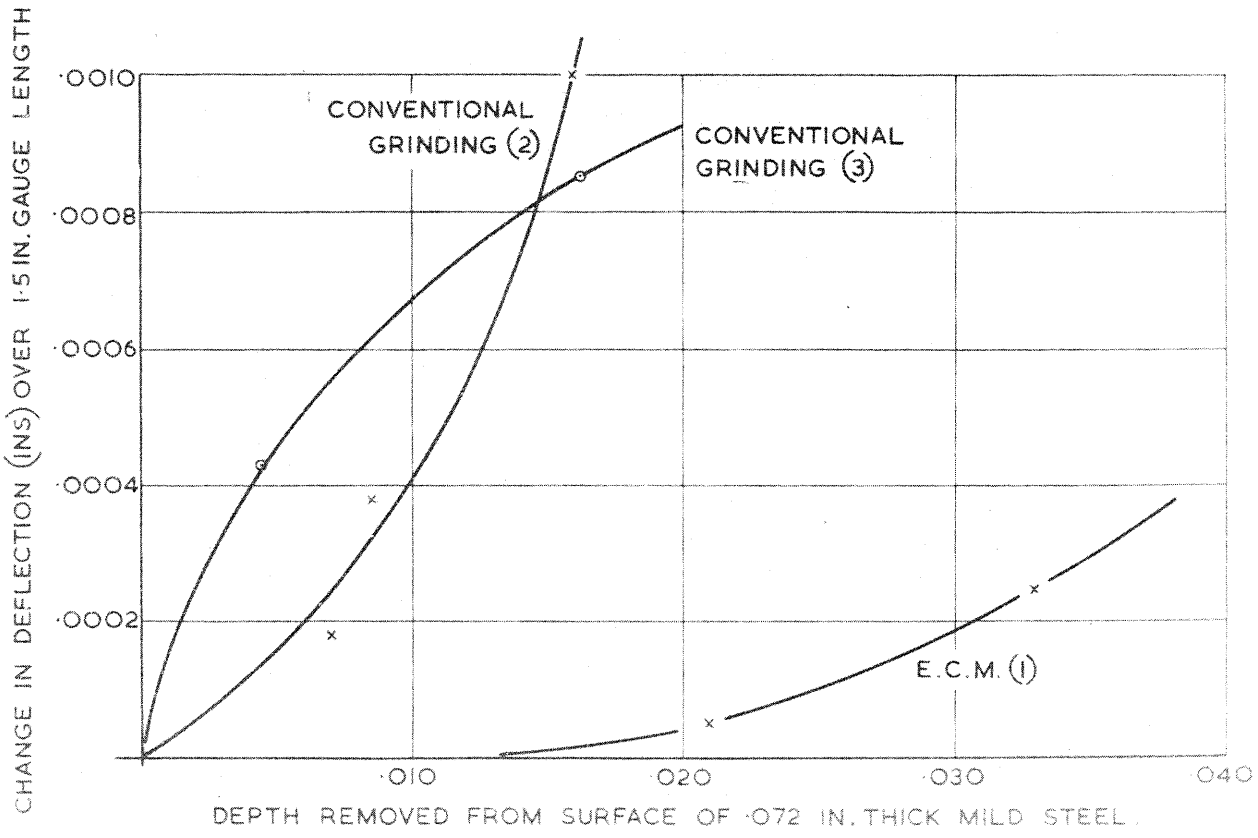

FIG. 23. CHANGE IN CURVATURE RESULTING FROM MACHINING MILD STEEL

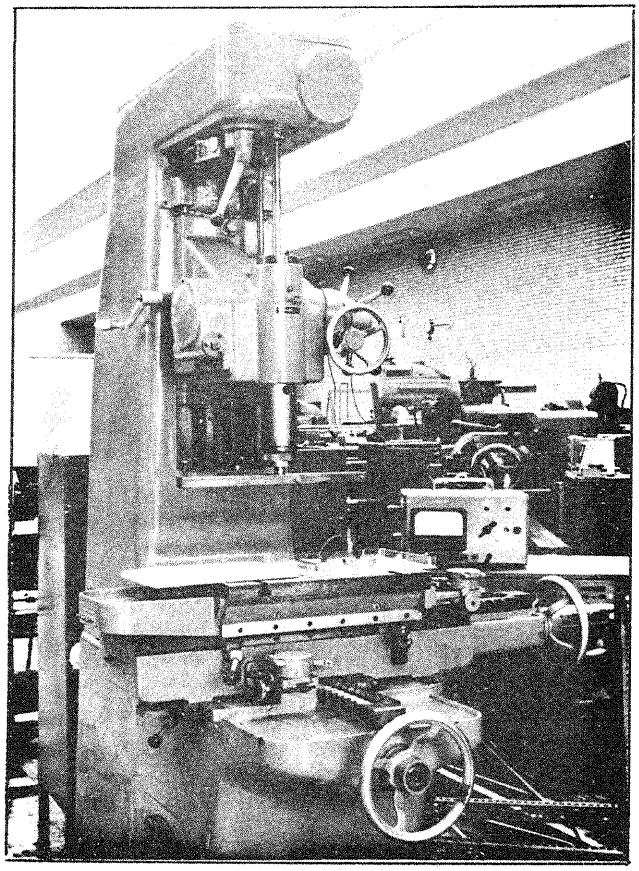

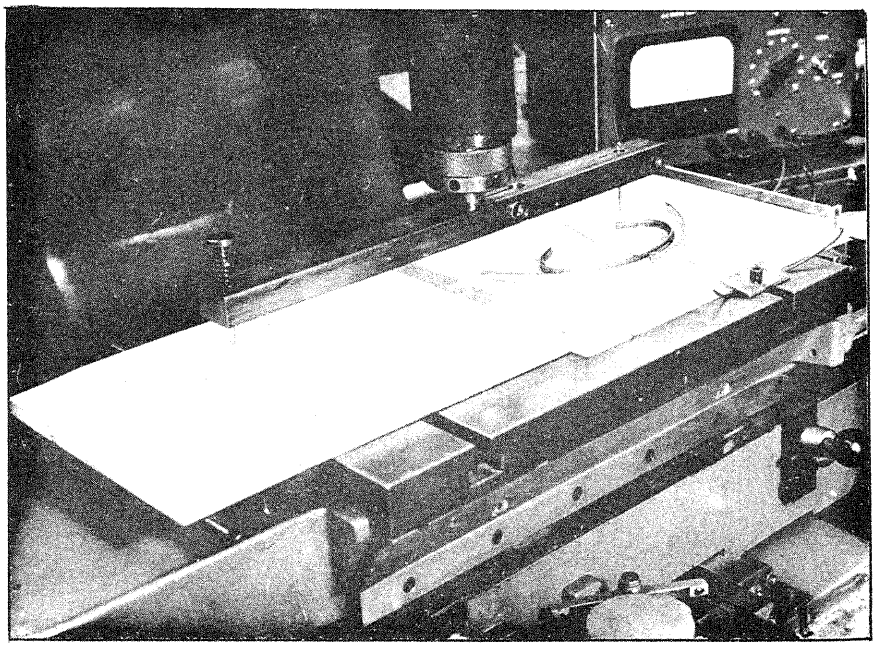

FIG. 24. STATIC FIELD PLOTTING EQUIPMENT ON NEWALL JIG BORING MACHINE

FIG. 25. STATIC FIELD PLOTTING TASKS AND RECORDING APPARATUS

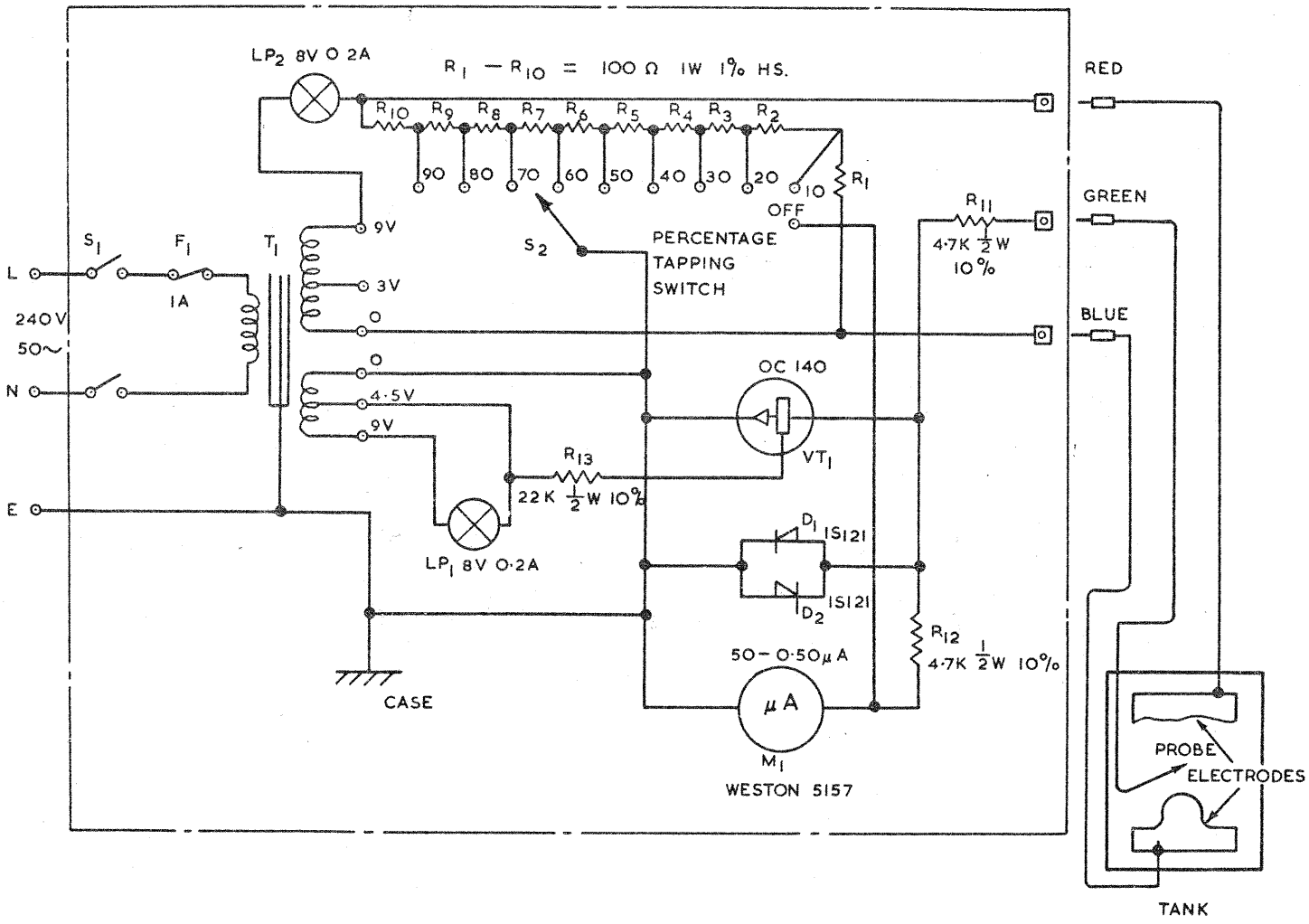

FIG. 26. ELECTRICAL CIRCUIT FOR A. C. BRIDGE UNIT

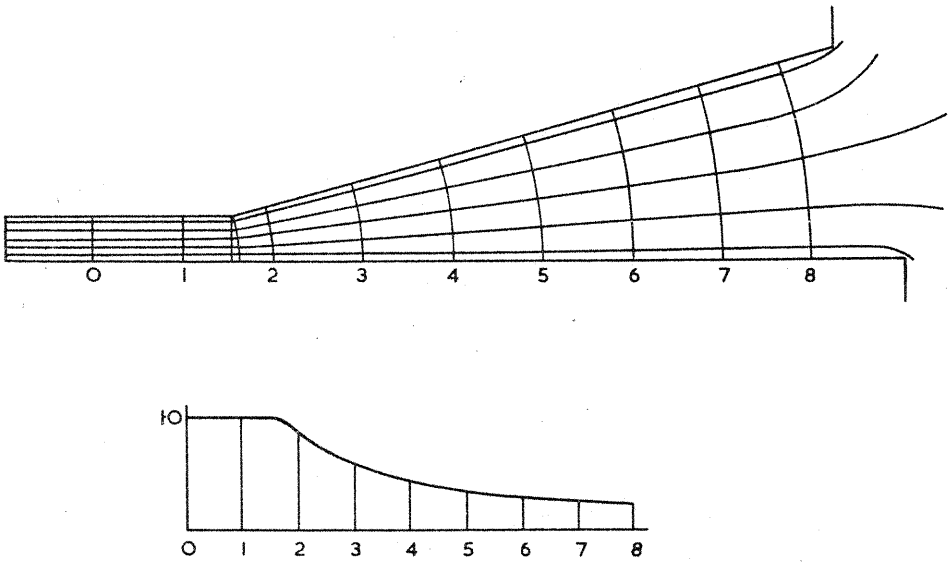

CURRENT DISTRIBUTION PATTERN

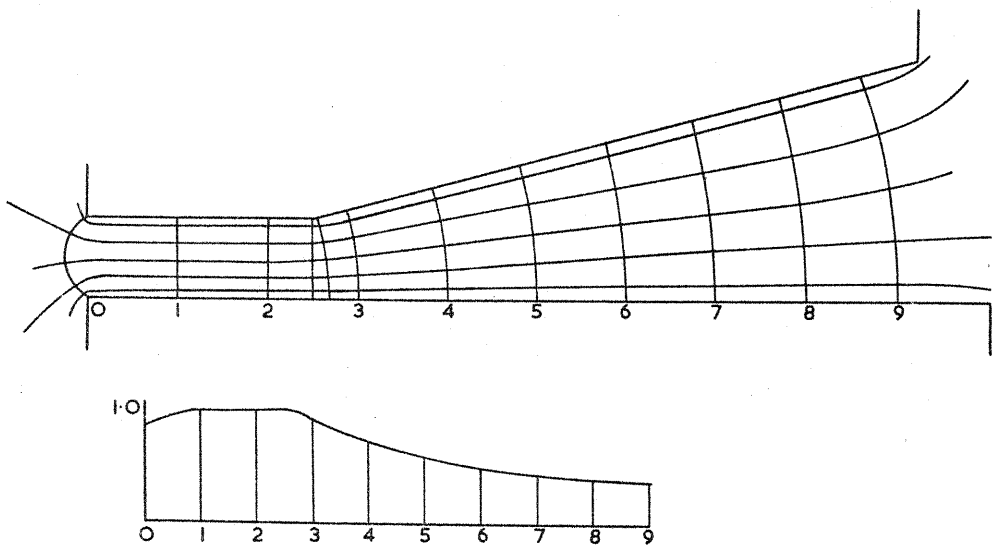

CURRENT DISTRIBUTION PATTERN

FIG. 27. STATIC FIELD AND CURRENT DISTRIBUTION FOR CHANGE IN GAP SIZE.

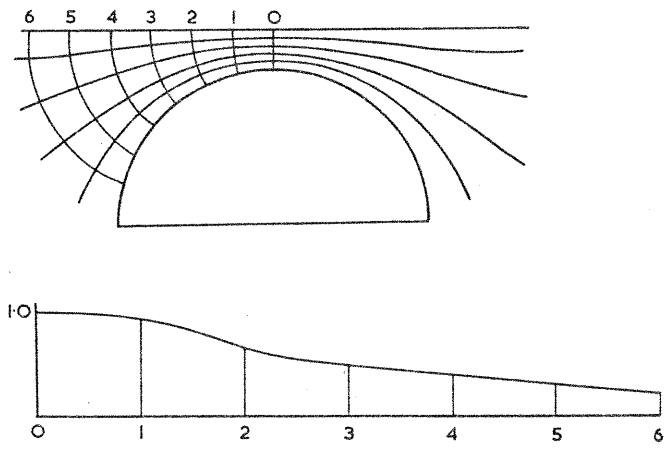

FIG. 28(a) STATIC FIELD AND CURRENT DISTRIBUTION FOR SEMI-CIRCULAR CATHODE AND FLAT ANODE - MAX. CURRENT DENSITY AT CENTRE.

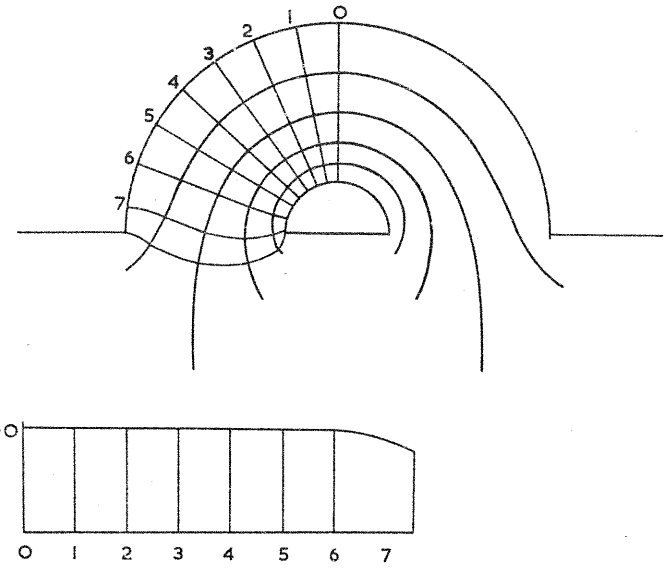

FIG. 28(b) STATIC FIELD AND CURRENT DISTRIBUTION FOR SEMI-CIRCULAR CATHODE AND ANODE - LARGE GAP

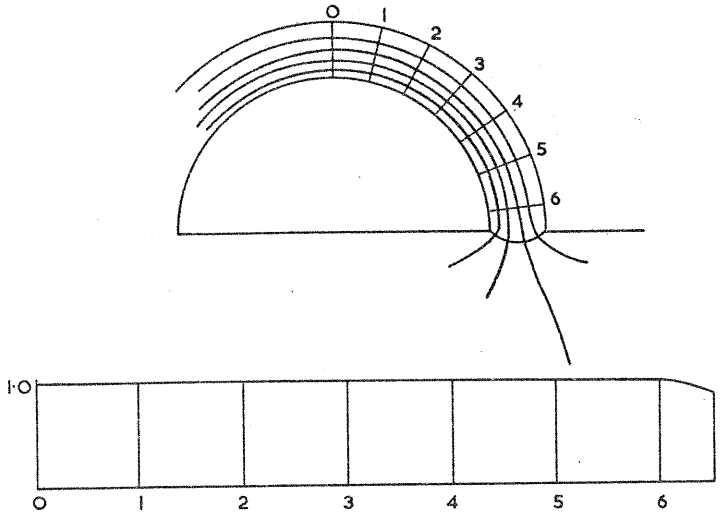

FIG. 28(c) STATIC FIELD AND CURRENT DISTRIBUTION FOR SEMI-CIRCULAR CATHODE AND ANODE - SMALL GAP

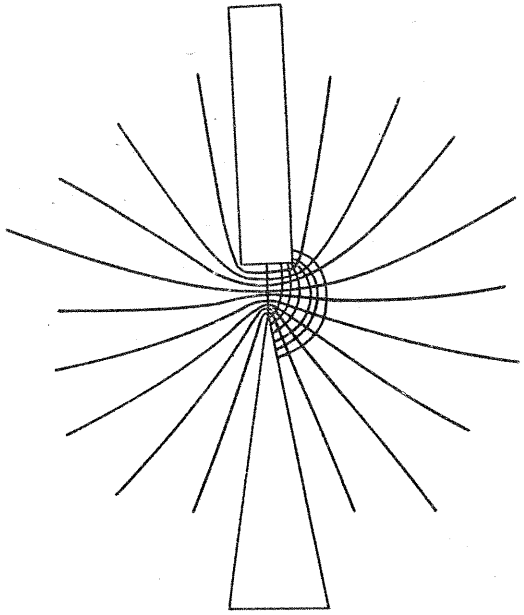

FIG. 28(d) STATIC FIELD FOR SQUARE ANODE, SHARP WEDGE CATHODE - NOTE CURRENT CONCENTRATION AT SQUARE EDGES

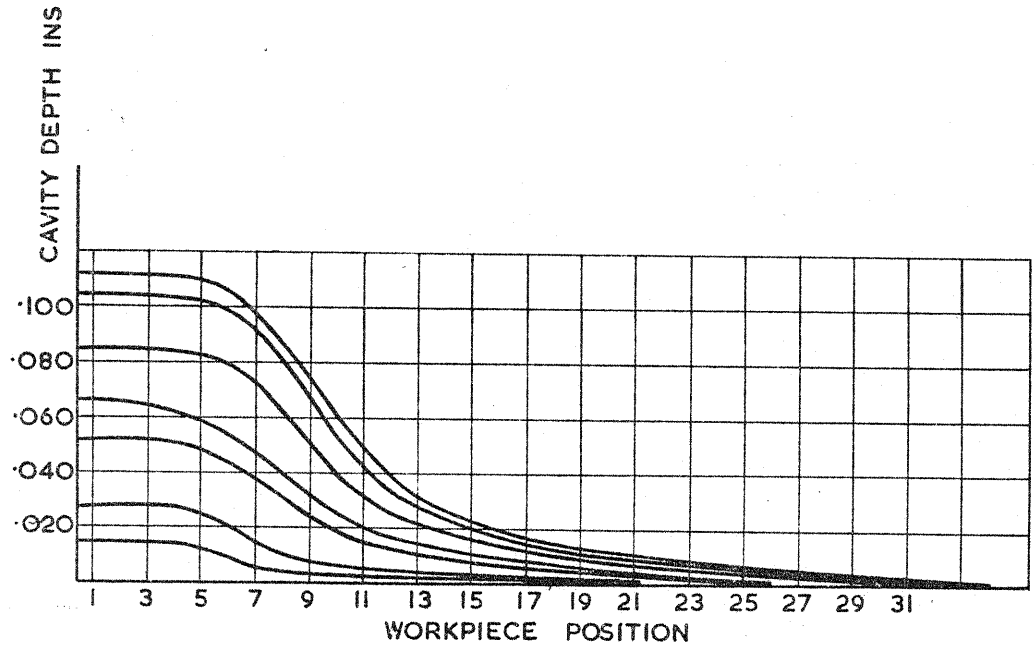

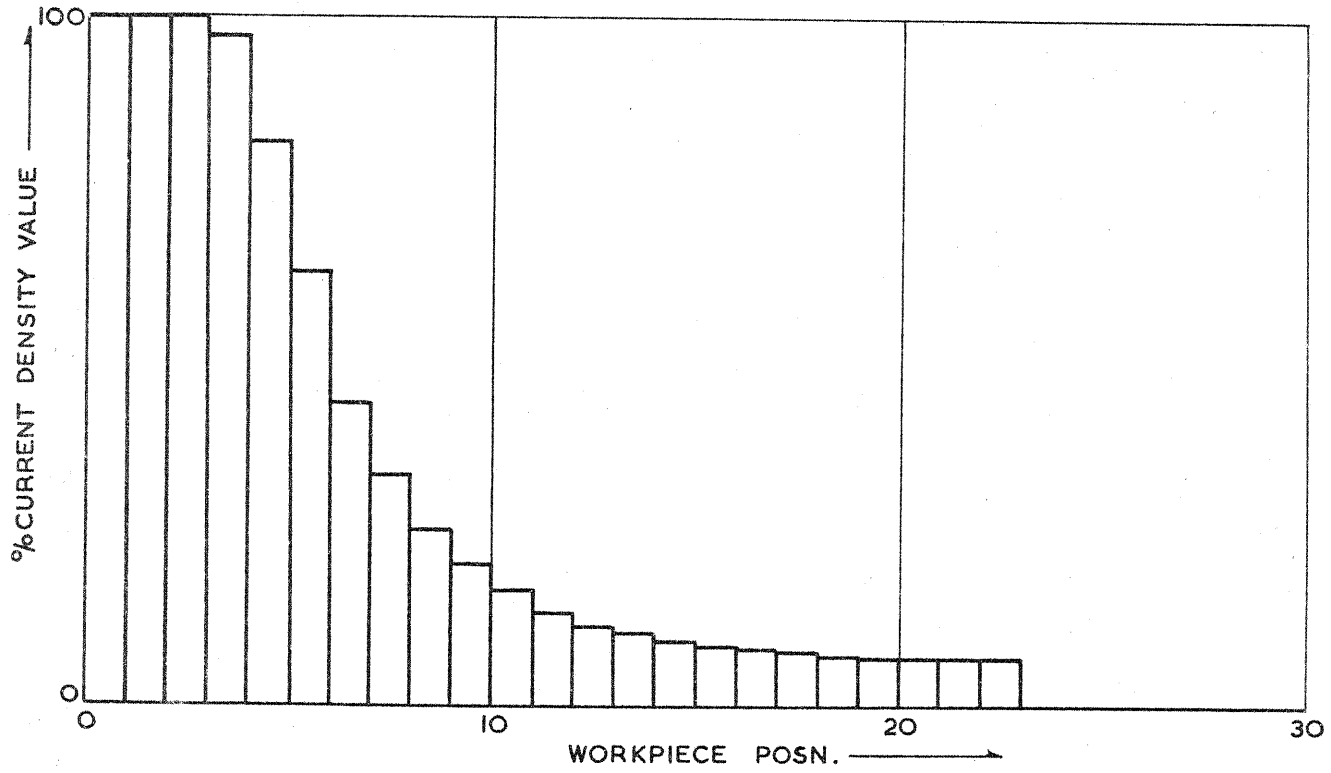

FIG. 29. PROGRESSIVE ANODE SHAPES WITH RECTANGULAR CATHODE DETERMINED FROM STATIC FIELD AT DISCREET TIME INTERVALS

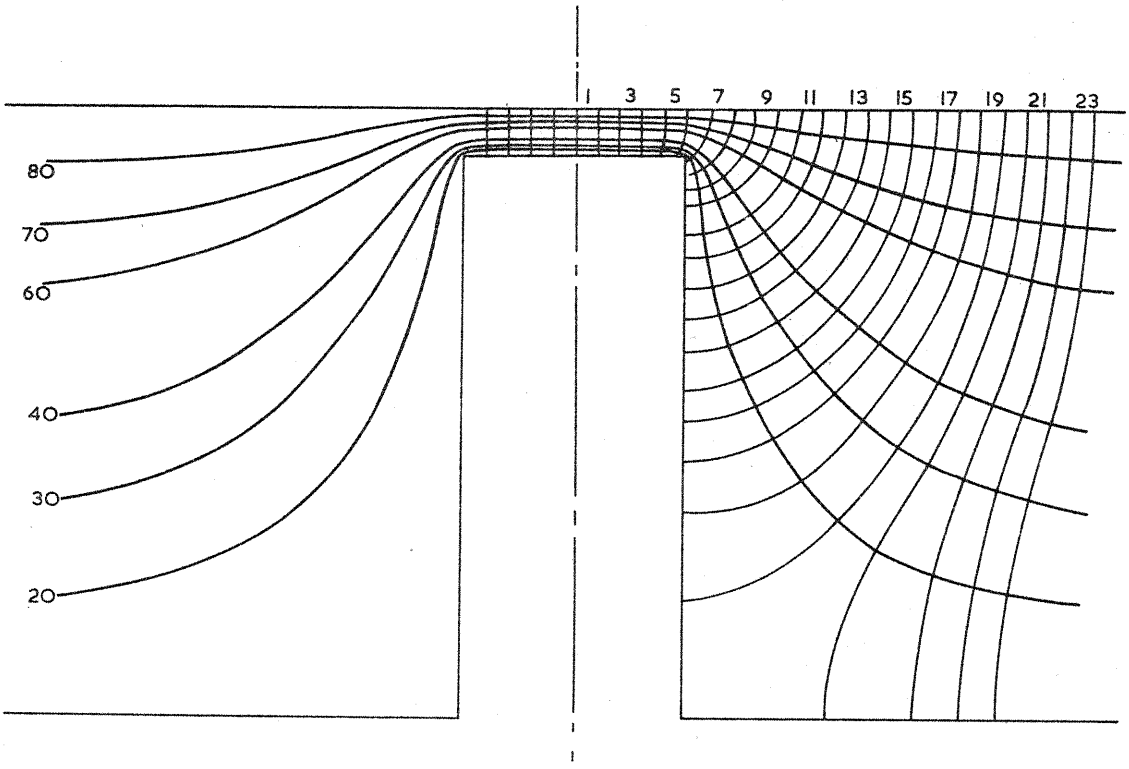

FIG. 30(a) STATIC FIELD FOR RECTANGULAR CATHODE AND FLAT ANODE

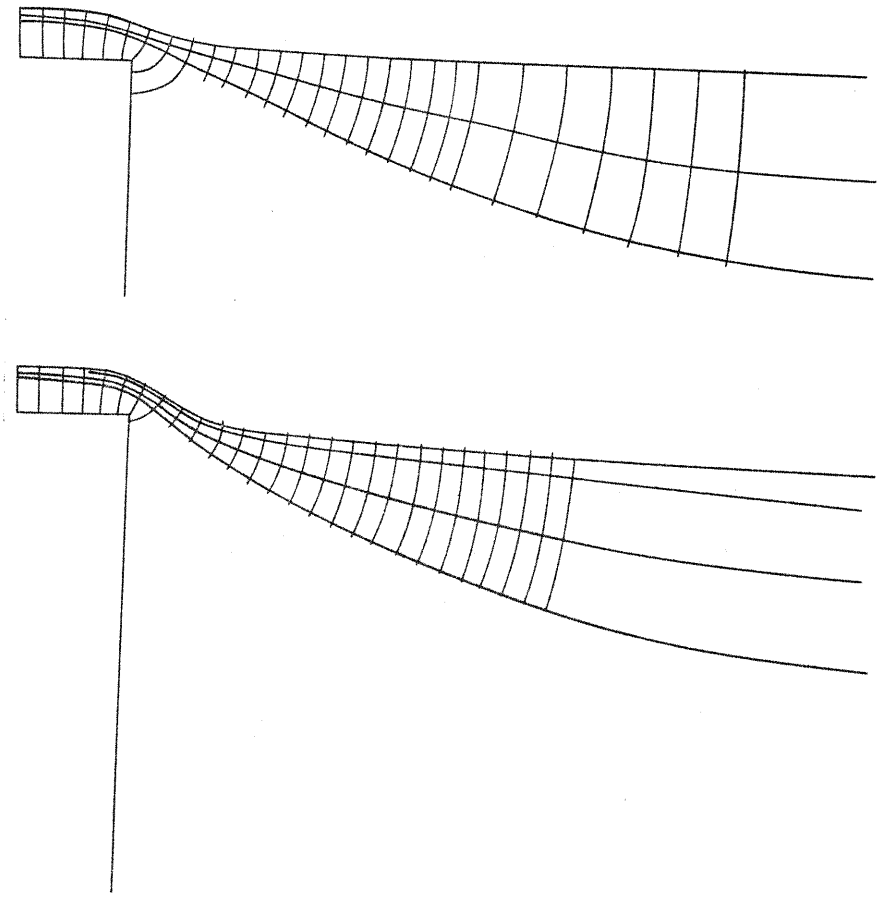

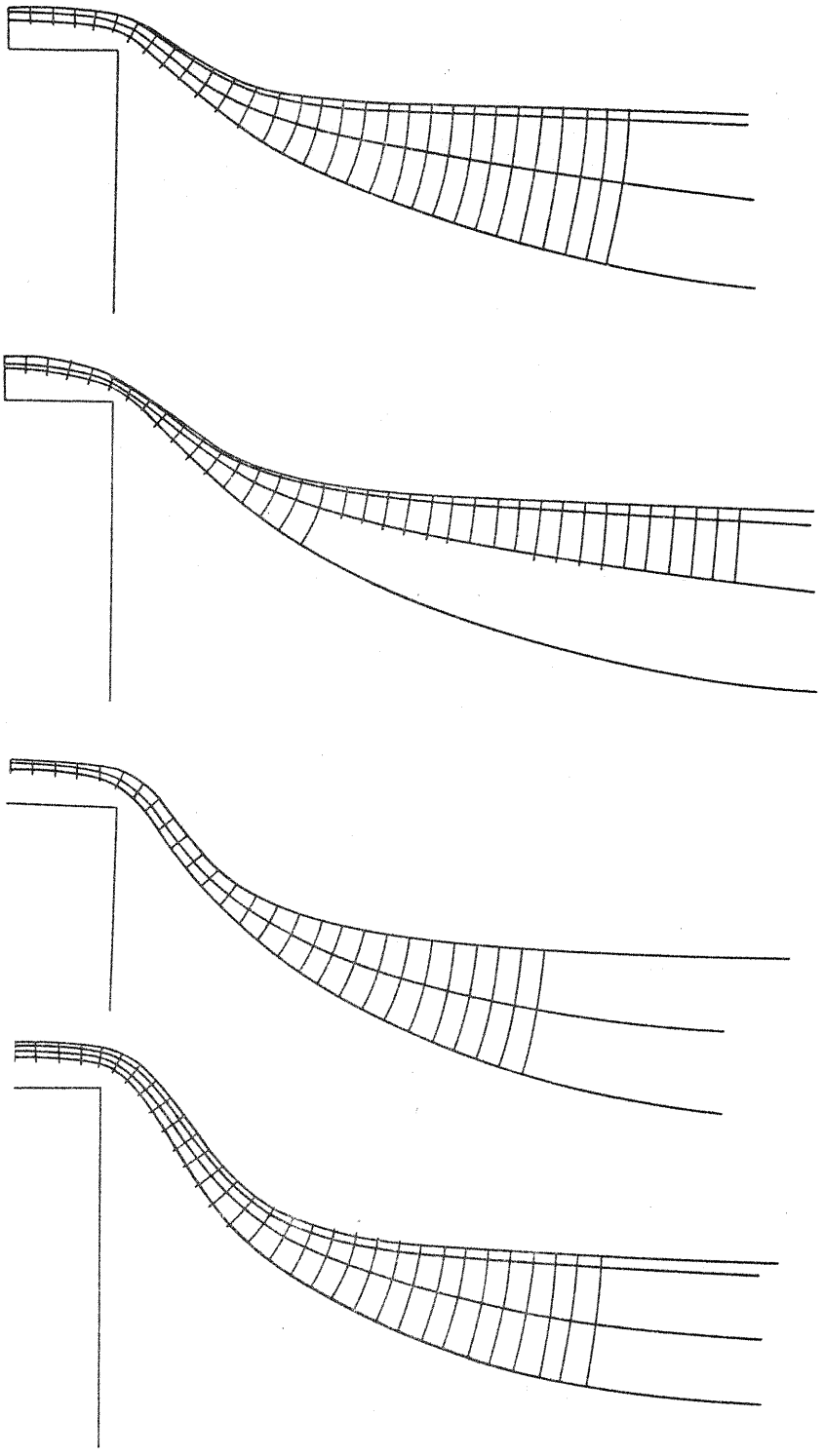

FIG. 30(b) PROGRESSIVE STATIC FIELDS WITH RECTANGULAR CATHODE

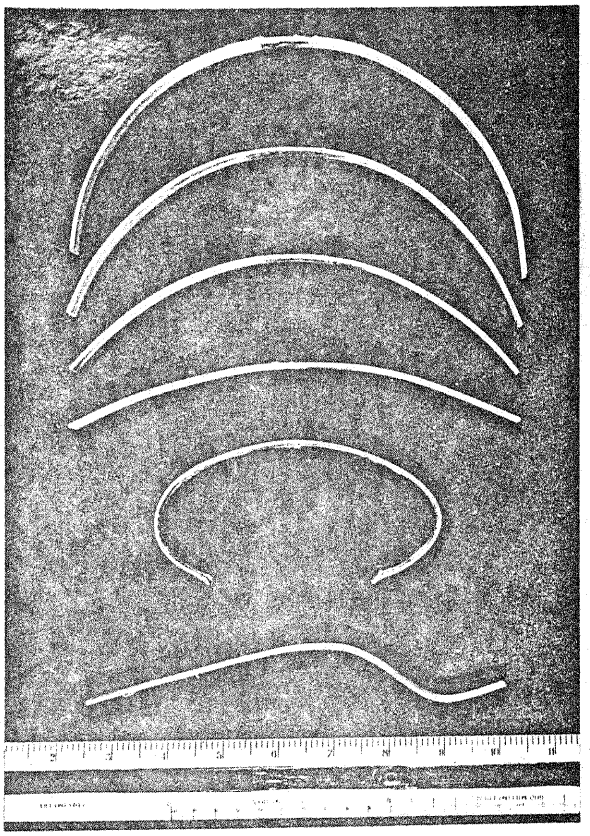

FIG. 31. SIMULATED ELECTRODE SHAPES FOR STATIC PLOTS

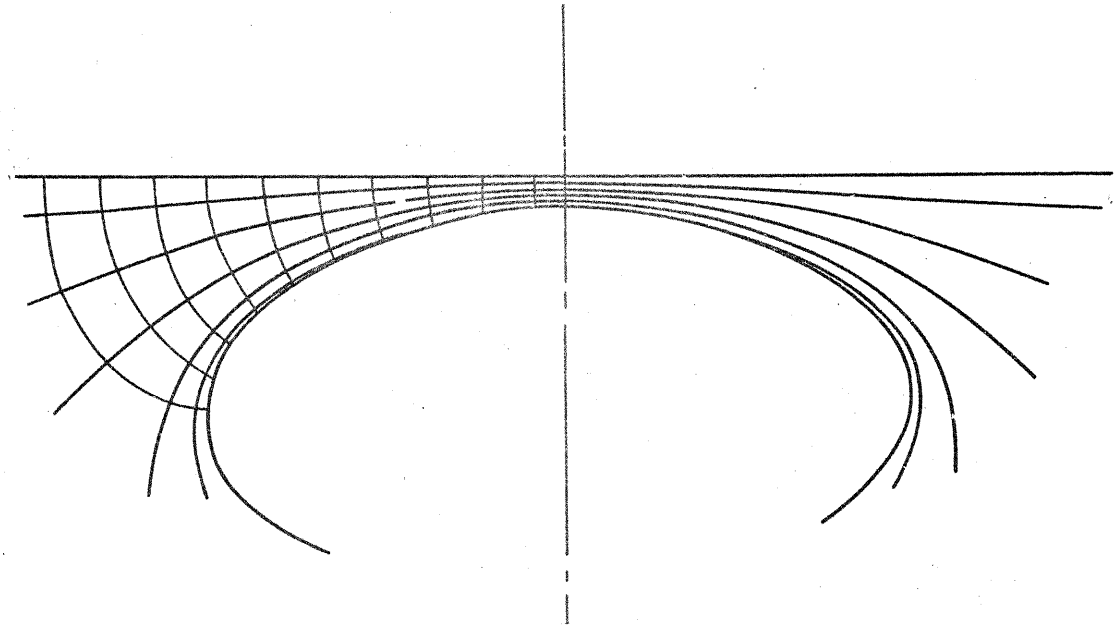

FIG. 32(a) STATIC FIELD WITH ELIPTIC CATHODE AND FLAT ANODE

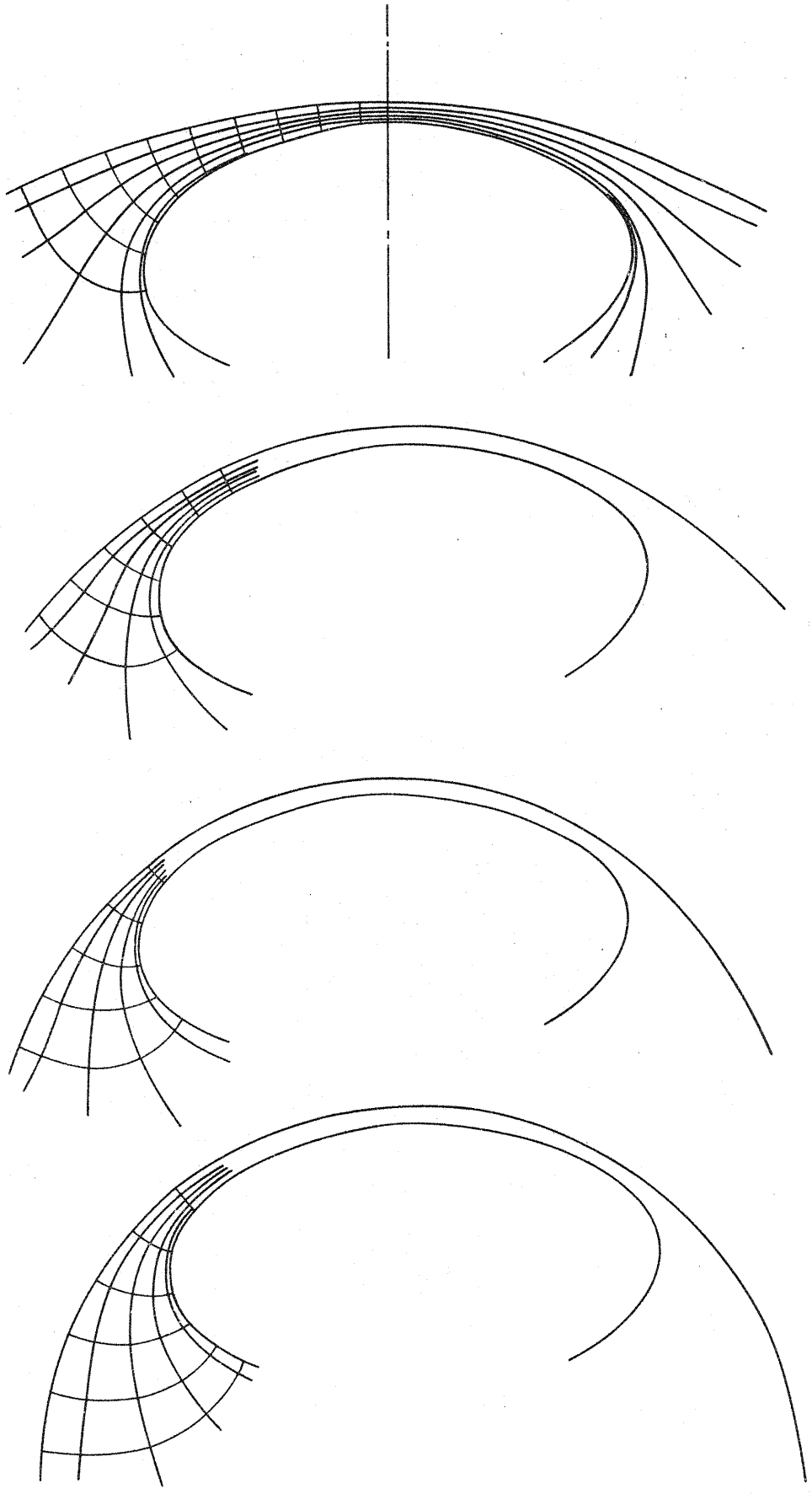

FIG. 32(b) PROGRESSIVE STATIC FIELDS WITH ELIPTIC CATHODE

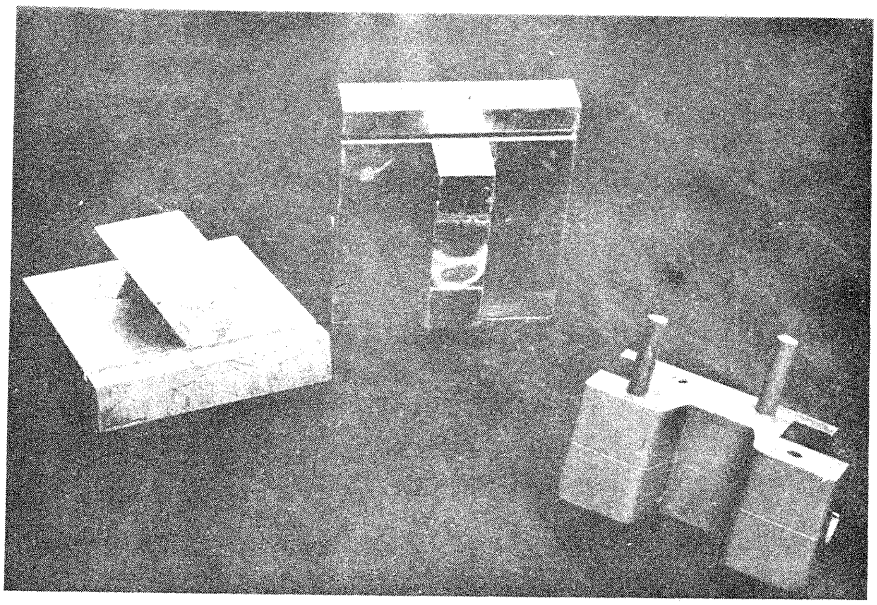

FIG. 33 TWO MACHINING CATHODES AND TYPICAL WORKPIECE

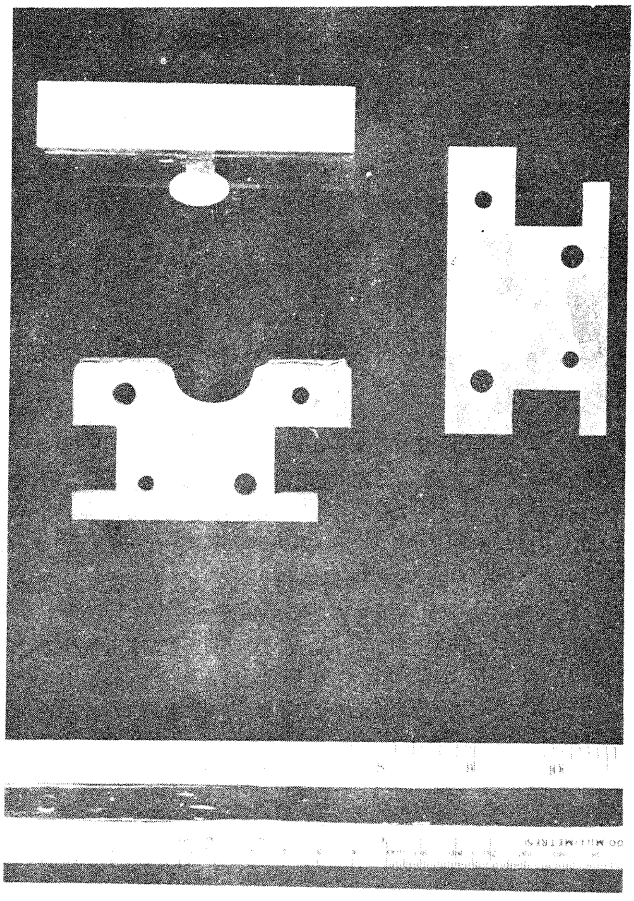

FIG. 34 ELIPTIC CATHODE AND WORKPIECE BEFORE AND AFTER MACHINING

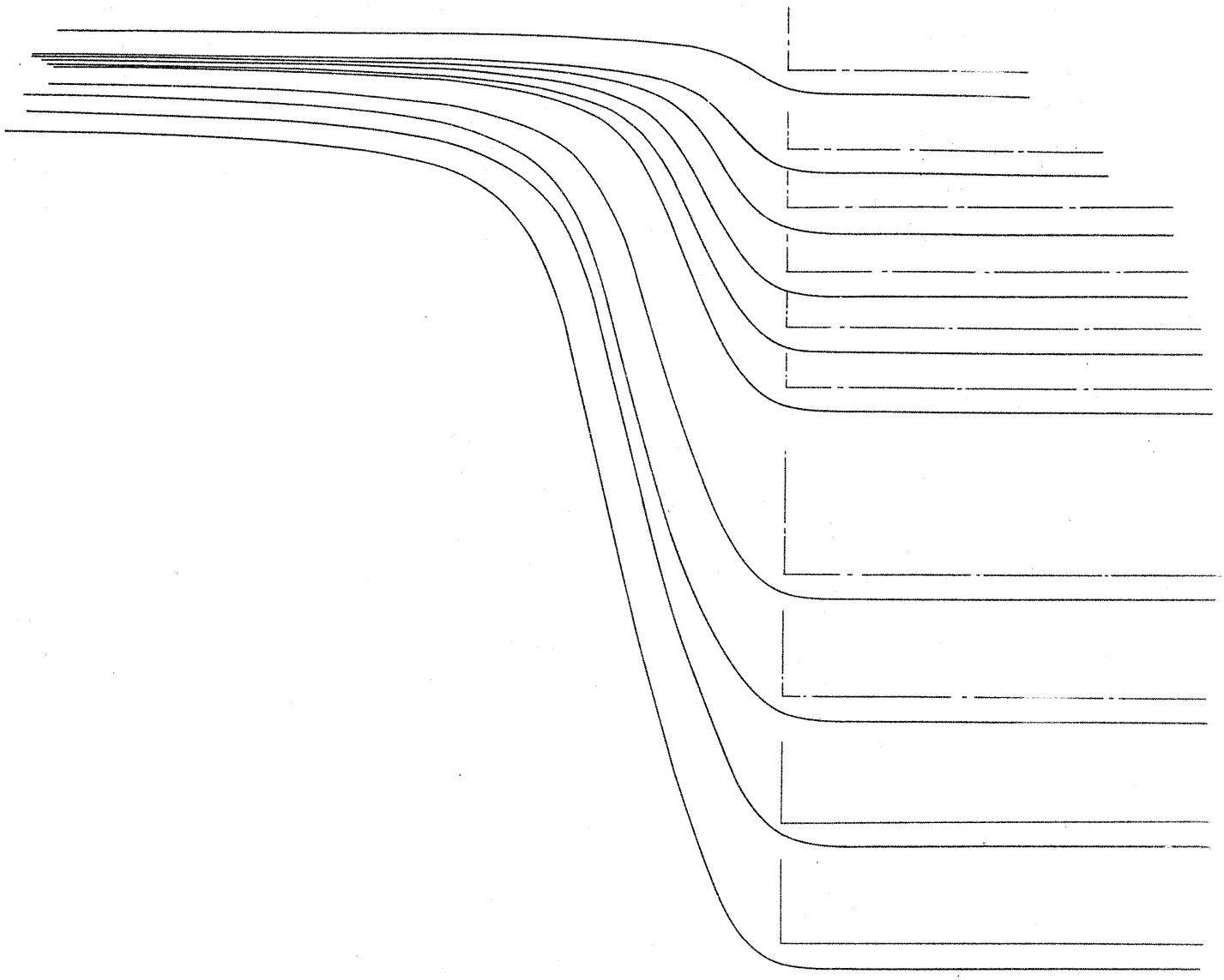

FIG. 35. WORKPIECE PROFILES DURING MACHINING

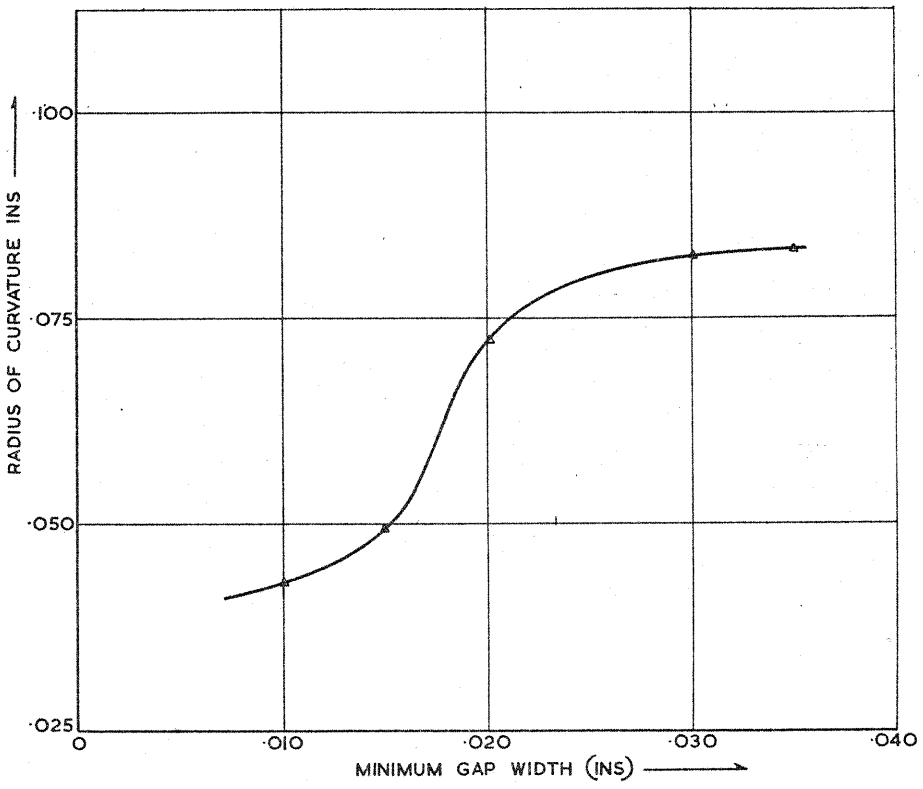

FIG. 36(a) WORKPIECE CORNER RADIUS, MINIMUM GAP RELATIONSHIP WITH RECTANGULAR CATHODE HAVING .012 EDGE RADIUS

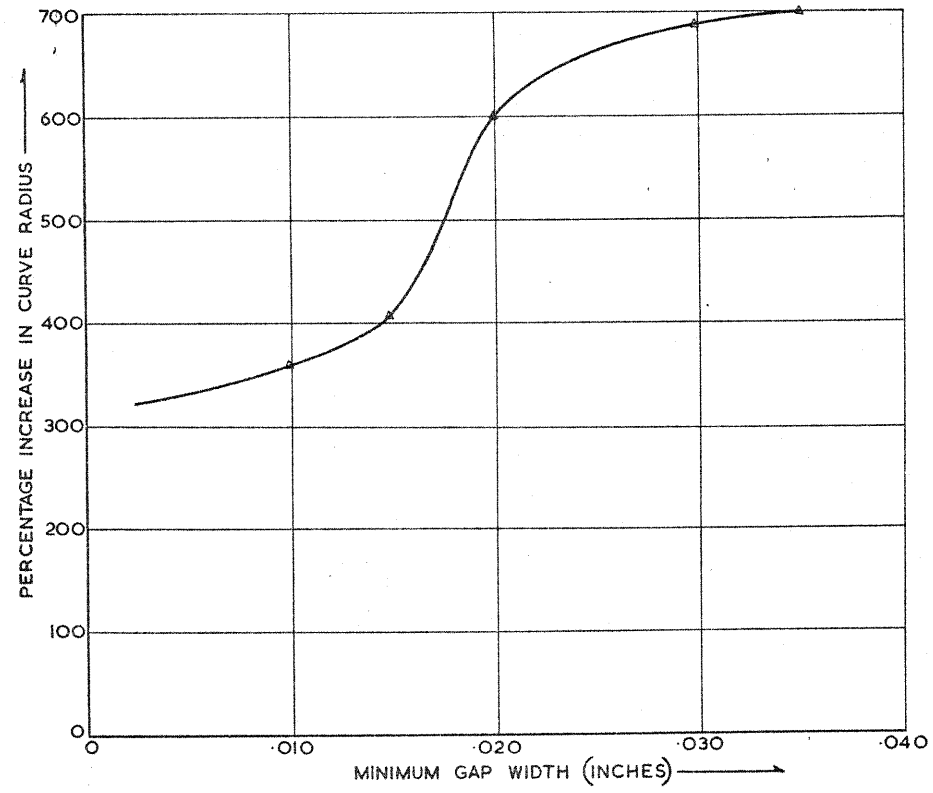

FIG. 36(b) PER. CENT WORKPIECE CORNER RADIUS TO CATHODE RADIUS WITH INCREASING GAP

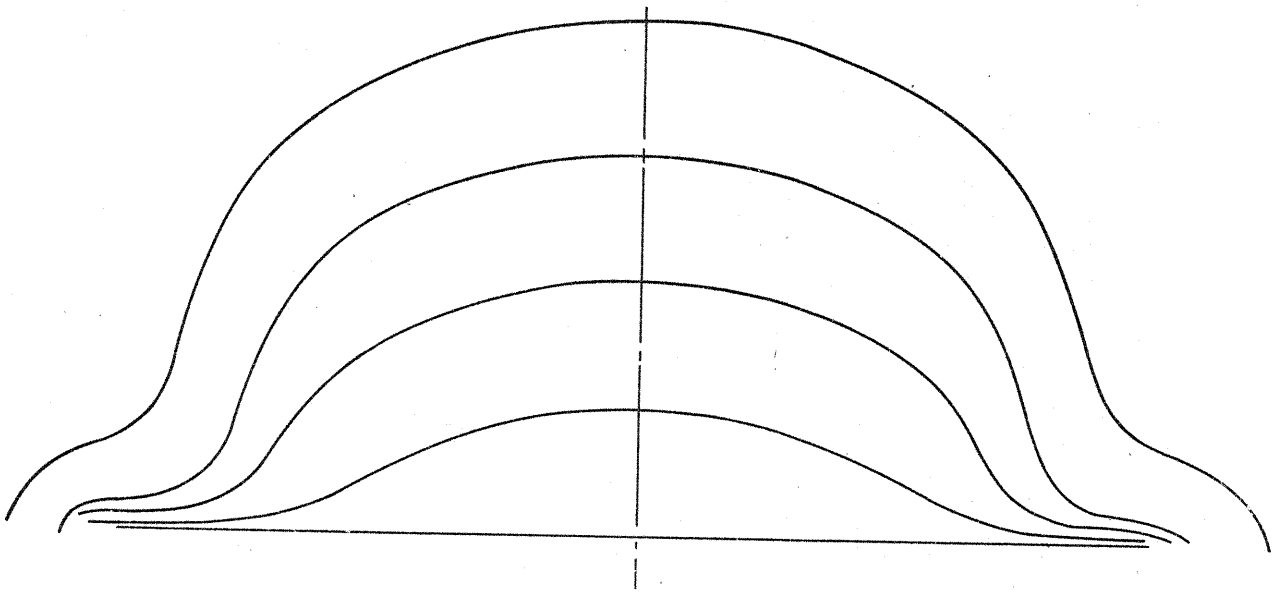

FIG. 37. WORKPIECE PROFILES DURING MACHINING WITH ELIPTIC CATHODE

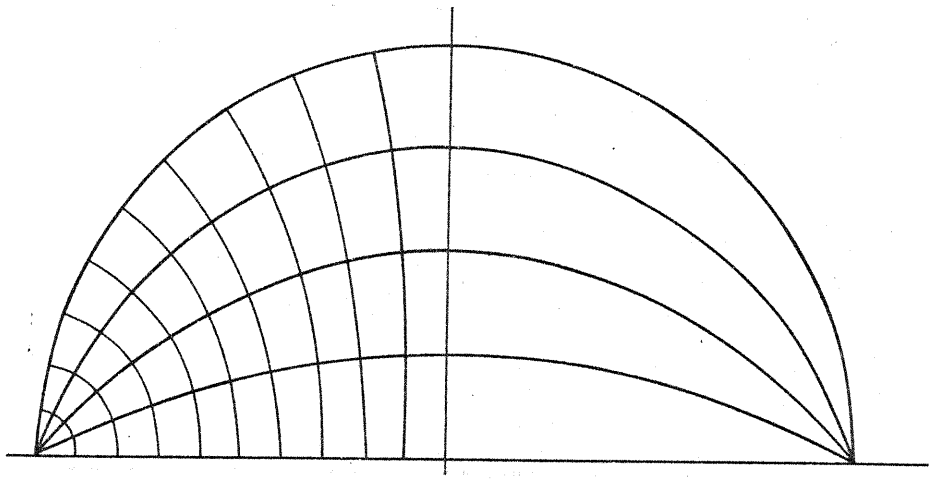

FIG. 38(a) IDEAL WORKPIECE PROFILES REQUIRED DURING MACHINING

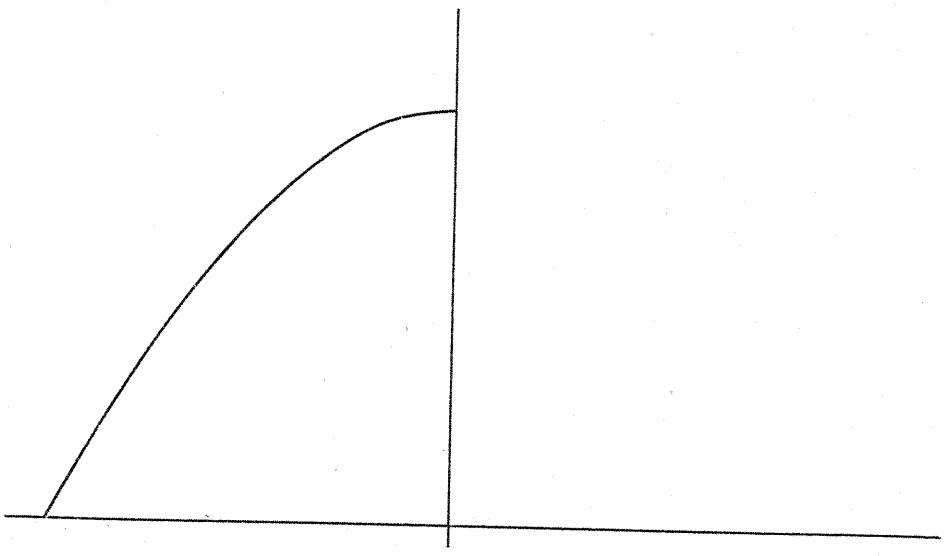

FIG. 38(b) CURRENT DISTRIBUTION REQUIRED TO OBTAIN IDEAL PROFILES (a)